Reference Code: hess-2018-393

Title: Spatially dependent Intensity-Duration-Frequency curves to support the design of civil infrastructure systems

Corresponding Author: Phuong Dong Le (The University of Adelaide)

Contributing Authors: Michael Leonard and Seth Westra

Response to the Reviewer #1

This manuscript describes the application of a correlation model for spatially dependent rainfall and hydrological response of four subcatchments that can cause flooding of a highway. The road is blocked if either of flows from the four subcatchments exceeds a critical threshold. The probability of system failure (road blockage) thus depends on the exceedance probability of four thresholds by four correlated stochastic variables.

Although the scientific methods that are used in this study may not be entirely new, the explanation of spatial dependency of rainfall and application to a practical case study are very clear and a pleasure to read. After reading this manuscript, a decision maker should understand that it is important to take this correlation into account.

I have only one specific comment: the core of the technical approach I would consider to be the correlation model, i.e. the Brown-Resnick inverted max-stable process. This method is not explained at all. Instead, the authors choose to refer to literature. Although a fully detailed description of the B-R algorithm may be too much, it would be good if the essence of this method is explained briefly.

Response: Thank you very much for your suggestion. Although a full explanation of the B-R model is very long and technical and well-covered in other papers, we have provided a brief summary of the main technique through the inclusion of a high-level algorithm in the next version of the manuscript.[1]

---

[1] Line 241: "An example of an asymptotically independent model is the inverted max-stable process (Wadsworth and Tawn, 2012). A general description of all continuous inverted max-stable processes that have standard exponential margins on a spatial domain X is

$$\widetilde{\Omega}(x) = \min_{k\geq 1} U_k / W_k\,, \quad x \in X, \tag{2}$$

where U_k are points of a unit Poisson process on $(0, \infty)$ and the $W_k(x)$ are independent replicas of a continuous, non-negative stochastic process $W(x)$ in the spatial domain X, with $E\{W(x)\} = 1$ for all $x \in X$.

It is convenient to work with a simple inverted max-stable process with unit Fréchet margins, because the marginal distribution can easily be transformed back to the GPD scale. To transform the process $\widetilde{\Omega}(x)$ to unit Fréchet margins, the following transformation is used:

$$\Omega(x) = -\frac{1}{\log\{1 - e^{-\widetilde{\Omega}(x)}\}}, \quad x \in X, \tag{3}$$

then $\Omega(x)$ is an asymptotically independent process with unit Fréchet margins."

Response to the Reviewer #2

The manuscript describes a statistical framework based on an inverted max-stable process allowing to account for the spatial dependence of rainfall across durations. Application is made for a case study in New South Wales, Australia. Using the proposed framework, the author are able to compute conditional and joint return levels of rainfall. Through the use of rainfall ARFs and of an hydrological model, that authors also derive conditional and joint return levels of river flows. Finally the authors derive the failure probability of a highway section, defined as the probability that flood magnitude at any of the five river crossings exceeds a given threshold, assuming a 1-1 correspondence between flood magnitude and rainfall over a catchment.

Main comments: The article is well written and mainly clear. The two risk applications of Section 5.1 and 5.2 are very interesting, particularly 5.2 (failure probability of a highway section) which seems to me to be more related to "real" issues than 5.1. The subject is absolutely worth publishing in HESS. However I raise below a couple of major issues to be addressed before publication:

Response: Thank you for your comments. We respond in detail below (your comments in italic font and our responses in normal font).

Major comment #1:

The use of "Intensity-Duration-Frequency curves" in the title seems at the moment misleading. I would have expected from this expression to see e.g. joint or conditional IDF curves at a given station/catchment, i.e. the IF curves for several durations. Here actually only one duration is used for every catchment – basically the concentration time of the catchment. So I'd be tempted to replaced "IDF" in the title (and the text) by "return levels".

Response: As the reviewer comments, the use of "Intensity-Duration-Frequency curves" suggests plots of IF with respect to duration, which we have not shown, and we instead showed return level maps. We propose to use "Intensity-Duration-Frequency relationships" in the title, since the method involves these three elements, but hopefully avoids the suggestion of traditional IDF curves.

The model can produce IDF curves at any given location as well as exceedance relationships of a conditional distribution. We have provided here an additional figure showing this relationship across multiple durations based on the example in Figure 10 of the existing manuscript which focused only on the 9-hour to 36 hour conditional relationship.

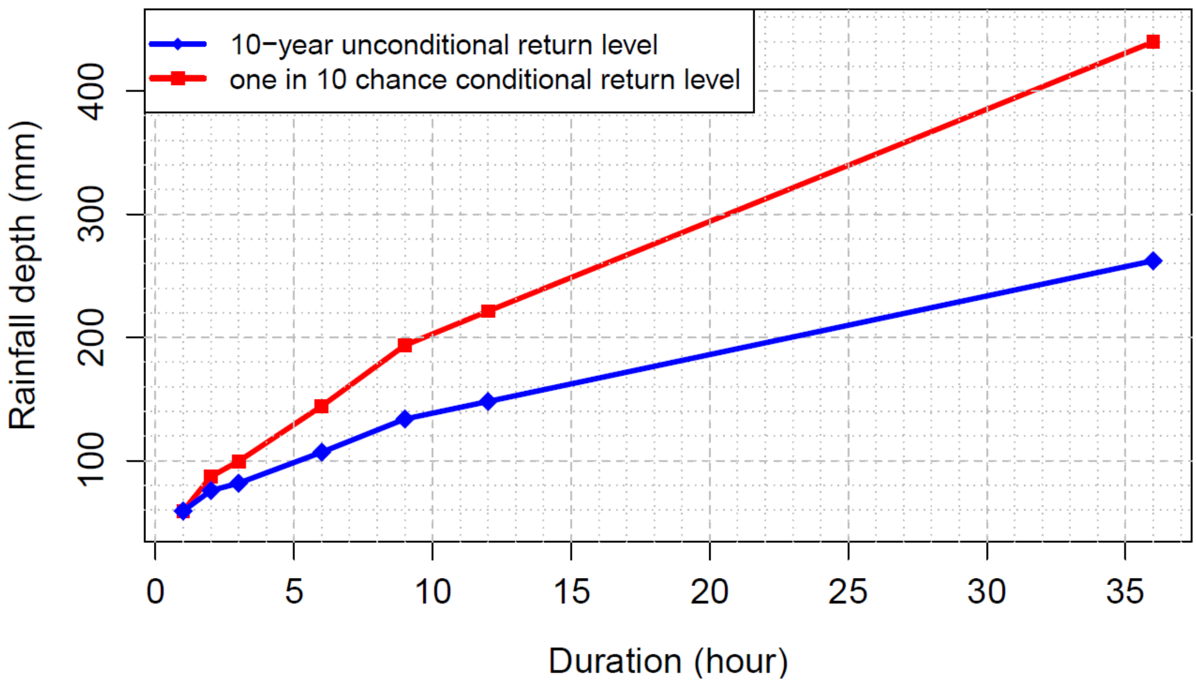

Figure R1. The exceedance relationship of a conditional distribution across multiple durations based on the example in Figure 8 in the manuscript. The blue line is the relationship between 10-year unconditional return levels (at the location of the blue star in Figure 8) and durations, and the red line is the relationship between one in 10 chance conditional return levels (at the location of the blue star in Figure 8) and durations, given a 20-year event for 36 hr extremes happens at location of the red star (in Figure 8) for the centroid of the Kalang River catchment.

Major comment #2:

I'm puzzled about the GPD fits. If I understood correctly, GPD are fitted to 9 and 36 hr rainfall exceedances. If moving windows are considered, then there is a very strong auto-correlation for both the 9 and 36 hr rainfall values. Have you taken this into account in the fits? A declustering method should be applied. This may be the reason why the fits for 36 hr extremes are usually poorer than for 9 hr extremes (see Figs S5 and S6).

Response: Thank you. We did not consider moving windows; instead, we used restricted time periods for 36 hr rainfall (e.g. 01/01 00:00 to 02/01 12:00; 02/01 12:00 to 04/01 00:00; …). The use of a restricted estimates avoids the need for declustering to undo the effect of a moving window. We used a conversion factor of 1.13 to account for the difference between sliding (unrestricted) *d* hr rainfall maxima and restricted *d* hr maxima. This value is based on guidance from Australian Rainfall and Runoff (where Table 2.3.4. from Green et al. (2016) gives the 24-hr factor as 1.15 and the 48-hr factor as 1.11).

Inside the 36 hr period we also restricted the period for 9 hr rainfall (e.g. 01/01 00:00 to 01/01 09:00; 01/01 09:00 to 01/01 18:00; …). This is to align concurrent occurrences of 36 hr and 9 hr rainfall when analysing the spatial dependence across durations. We also used a conversion factor of 1.13 for this period (Figure 5 from Jakob et al., (2005) suggests the fitted conversion factor is relatively stable).

Regarding the fits to the 36 hours extremes, the shape parameter of the GEV has greater uncertainty for some sites (e.g.Fig S5, site 3, 36 hours) which can be seen in the deviations of the observed points from gumbel quantiles. Explanation for variability is unclear to us, but we do not consider it is related to temporal dependence in the extremes.

References used for this response:

Green J, Johnson F, Beesley C, The C, 2016, Chapter 3. Design Rainfall, Book 2 in Australian Rainfall and Runoff - A Guide to Flood Estimation, Commonwealth of Australia

Jakob D., Taylor B.F. and Xuereb K.C. (2005). A Pilot Study to Explore Methods for Deriving Design Rainfalls for Australia - Part 1., HRS No. 10, Hydrometeorological Advisory Service, Bureau of Meteorology, June 2005, (59 pp). http://www.bom.gov.au/water/designRainfalls/hrs10.shtml

Major comment #3:

The part regarding the ARFs seems obscure to me (Section 4.5). Basically I isn't clear tome what the ARF allow for. I interpret between the lines that they allow to transform point return levels to spatial return levels over a catchment. However the way ARFs are described is very confusing to me. For example l. 346 states that "the rainfall extremal estimates need to be converted to the average spatial rainfall using an ARF". First I don't understand what are the "rainfall estimates" (rainfall return levels?). Second I guess that " average spatial rainfall" should be "spatial rainfall return levels". I recommend clarifying Section 4.5 and part of the Introduction dealing with ARFs.

Response: Areal reduction factors (ARFs) were employed to make the adjustment of rainfall depth at a point for a given return level estimate, to an effective (mean) depth over a catchment with the same probability of exceedance as that of the point extreme (Le et al., 2018).

We have clarified the text relating to the explanation of ARFs based on your observations.[2]

References used for this response:

Le, P. D., Davison, A. C., Engelke, S., Leonard, M., and Westra, S.: Dependence properties of spatial rainfall extremes and areal reduction factors, Journal of Hydrology, 565, 711-719, https://doi.org/10.1016/j.jhydrol.2018.08.061, 2018.

Major comment #4:

Expressions such as "10-year conditional return level map given a 20-year event happen at x" are confusing to me. Wouldn't it be less confusing to say this is the levels. expected to occur on average once every 3650 times when a 20-year event happen at x. The "10-year" is misleading to me in that case due to the conditioning.

Response:

On review, we agree that this terminology of return periods is misleading. Our general design intent is introduced as: "What flood flow needs to be used to design a bridge that will fail only once on average every M times that a neighbouring catchment is flooded?" However, we then suggested that if M=10 this

[2] Line 332: "Before transforming extreme rainfall to flood flow through an event-based model, areal reduction factors (ARFs) were employed to make the adjustment of rainfall depth at a point (i.e. the centroid of a catchment) for a given return level estimate, to an effective (mean) depth over a catchment with the same probability of exceedance as the single point (Ball et al., 2016; Le et al., 2018a)."

implies a 10-year event. On review, we see the use of return periods is confused and are grateful the reviewer has raised the matter.

For the example of daily events (365 days per year), a 10% exceedance of a conditional distribution cannot be used to imply there were 10 years equivalent or 3650 instances – because the condition only applies to a subset of days. As the reviewer has indicated, a descriptive frequency is more transparent and we will remove all instances referring to conditional “return periods”. We have exclusively retained descriptive phrases such as “once on average every M times” or “one in M chance” in discussion, figure labels and figure captions.

Major comment #5:

I’m confused with the reference to “annual maxima”, whereas the article considers peaks-over-threshold. For example Fig 1 illustrates the case of annual maxima (GEV), which is not the case here. L. 421-423 talks about annual maxima instead of exceedances.

Response: Thank you for pointing this out. We use the peaks-over-threshold model in this paper. So we have fixed the text in L. 421-423, they should be exceedances. We used Fig 1 to shows the limitation of the conventional method so the fact that Fig 1 illustrates the case of annual maxima (GEV) is correct.

Major comment #6:

I haven’t understood what is the AEP of Fig 12 and 13. I guess it would be clearer to replace AEP by return periods.

Response: The reviewer is correct that it is not clear what an AEP means for a conditional distribution (as with Major comment #4 for return periods). For example, a 10% chance of exceedance in a conditional distribution is not a 10% *annual* exceedance. For this reason, Fig. 12 is confusing and we have removed it along with associated discussion. The use of AEP in Fig. 13 is correct and we still retain it.

Minor comment #1:

l. 111: Le et al → no brackets.

Response: Thank you. We have fixed this.

Minor comment #2:

l. 113 AFR → ARF

Response: We have fixed this. Thanks.

Minor comment #3:

l. 116-117: I may be clearer to exemplify (i) in terms of evacuation route design as you do in Section 5.1.

Response: The phrase in question is: "*What flood flow needs to be used to design a bridge that will fail only once on average every M times that a neighbouring catchment is flooded?*"

As with the response to major comment #4, we have addressed the main ambiguity by removing the invalid reference to return periods. Whereas the evacuation route is a general example, phrasing the research question this way allows us to introduce the need for a probability into the design specification.

Minor comment #4:

Fig. 3: add the station numbers 1, 2, 3...

Response: We have fixed this. Thanks.

Minor comment #5:

Fig. 4 estimate conditional rainfall $\rightarrow$ estimate conditional probability rainfall

Response: We have fixed this. Thanks.

Minor comment #6:

l. 277: where $\rightarrow$ to be removed

Response: We have fixed this. Thanks.

Minor comment #7:

l. 294-296: why don't you estimate all parameters (beta, q, c) together?

Response: This method is adopted from the paper of Le et al. (2018). If we fit all parameters ($beta$, q, and c) jointly, there will be a bias in the estimated c parameter because of the dominance of data points at longer distances, which underestimates the tail dependence coefficients at short distances. The main interest is in short distances, especially at $h = 0$ for the case of dependence between two different durations at the same location (see Figure 8 in the manuscript). Therefore, we estimate beta and q first, and then we use fitted $beta$ and q to estimate c.

References used for this response:

Le, P. D., Leonard, M., and Westra, S.: Modeling Spatial Dependence of Rainfall Extremes Across Multiple Durations, Water Resources Research, 54, 2233-2248, doi:10.1002/2017WR022231, 2018.

Minor comment #8:

l. 333-334 it is also noted .. 9 hrs $\rightarrow$ is it useful here?

Response: Yes, it is useful because it indicates that we need to analyse extreme rainfall for different durations.

Minor comment #9:

Section 4.5: to be rewritten to clarify the ARFs as said above

Response: Thank you. We have clarified this.

Minor comment #10:

l. 346: rainfall estimates: what are they?

Response: Thank you. We mean the extreme rainfall intensities at a given location, quantile and duration. We have fixed this in the updated manuscript.

Minor comment #11:

l. 353-354: the BR process → for what duration? With which parameters?

Response: In this paper, we need to calculate areal reduction factors for rainfall of 36 h and 9 h, so we only need to do the simulations for 36 h and 9 h separately. The parameters used are those for the variograms in Eq. (3) for rainfall of each durations, which is $\gamma(h) = ||h||^{\beta}/q$ for $q > 0$ and $\beta \in (0,2)$. So we need to fit Eq. (3) separately to observed rainfall of 36 hr and 9 hr to get the fitted parameters. We have provided the explanation for this in the revised version of the manuscript.[3]

Minor comment #12:

l. 360: empirical distributions → I'm confused here. If you use empirical distributions below the threshold, how can you have rainfall at ungauged sites (maps)?

Response: Thank you for your comment. The empirical distributions at ungauged sites are derived through the following steps:

- Step 1: We use a response surface for threshold for the case study catchments based on covariates including longitude and latitude.
- Step 2: We use the data of the nearest gauged sites and extract the empirical distributions of rainfall below the interpolated threshold in Step 1.

This method is not perfect, but we think that this is acceptable for this study, and for studies of extremes in general because the non-extremes contribute insignificantly (Thibaud et al., 2013). We have improved the explanation in the revised version of the manuscript.[4]

References used for this response:

---

[3] Line 341: "The simulation procedure for spatial rainfall for a given duration is implemented in two steps. In the first step, the theoretical residual tail dependence coefficient function in Eq. (5) is fitted to observed rainfall for the duration of interest to obtain the variogram parameters $q > 0$ and $\beta \in (0,2)$."

[4] Line 349: "The empirical distributions at ungauged sites are derived from the nearest gauged sites using a response surface (latitude and longitude covariates) to spatially interpolate the threshold."

Thibaud, E., Mutzner, R., and Davison, A. C.: Threshold modeling of extreme spatial rainfall, Water 737 Resources Research, 49, 4633-4644, 2013.

Minor comment #13:

l. 373: multiple durations → Is the algorithm of Dombry still applicable in this case? I'm not sure to see how it works for multiple durations.

Response: Yes, we think the algorithm of Dombry works properly for multiple durations in the following way. The covariance matrix of the simulation procedure provided by Dombry is calculated from the variogram in Eq. (4) of our paper. The covariance element for a pair of locations with the same duration (e.g. 36 and 36 hr) is calculated from the variogram of identical durations for 36 and 36 hr. The covariance element for a pair of locations with different durations (e.g. 36 and 9 hr) is calculated from the variogram across durations for 36 and 9 hr.

References used for this response:

Dombry, C., Engelke, S., and Oesting, M.: Exact simulation of max-stable processes, Biometrika, 103, 303-317, 2016.

Minor comment #14:

l. 373 in this case... pair of locations → I don't understand it at all. What covariance matrix are you talking about?

Response: This comment follows from minor comment #13, indicating that we have been ambiguous in this part of the method. We will improve the text to be clearer about how the covariance matrix is constructed.

Minor comment #15:

l. 378 rainfall hyetographs → what rainfall are you talking about? Spatial rainfall over the catchments?

Response: In event-based design methods, template rainfall hyetographs are applied to the areal rainfall total of a catchment for a specified frequency and duration. We have added a brief explanation and reference to design guidelines in the revised version of the manuscript.[5]

Minor comment #16:

Fig. 6: is it useful here? It could be in the supplementary material.

Response: We will move it to the supplementary material.

Minor comment #17:

[5] Line 377: "WBNM calculates flood runoff from rainfall hyetographs that represent the relationship between the rainfall intensity and time (Chow et al., 1988)."

l. 385 & 387: hydrological models → hydrological model layouts

Response: We will fix this when revising the manuscript.

Minor comment #18:

l. 398: did you apply declustering before estimating the GPDs?

Response: In short, we used estimates based on restricted totals (rather than a moving window) and did not apply declustering. Please also see our response to your major comment #2.

Minor comment #19:

Fig. 7 and SM: there is a huge difference between the extremes at the different stations, e.g. station 2 vs station 6. Could you comment on this? Also what method did you use to produce the confidence bands?

Response: Yes, there is a difference between the extremes at different stations. We can comment on this in the paper. We appreciate it is possible to improve the spatial model with additional covariates (and/or additional data such as daily rainfall observations), but the fidelity of the spatial model is not the main focus of the paper. We feel that the case study is sufficiently plausible to introduce the idea of conditional and joint relationships in hydrologic design.

We used the CAR package in R (qqPlot function). This function produces the confidence bands based on the SEs of the order statistics of an independent random sample (Fox, 2015).

References used for this response:

Fox, J., 2015. Applied regression analysis and generalized linear models. Sage Publications.

Minor comment #20:

l. 421-423: I'm lost here. Do you fit the BR process to annual maxima or exceedances?

Response: Thank you for pointing this out. We fit the BR process to exceedances. We have addressed this in the updated manuscript.[6]

Minor comment #21:

Caption of Fig 8: Abbreviation TDC is useless

Response: Thanks, we have fixed this.

---

[6] Line 419: "This is expected, as the dependence at the same site between exceedances at different durations will be lower than between exceedances at the same duration. This is because exceedances of different durations may arise from different storm events (Zheng et al., 2015)."

Minor comment #22:

Fig. 9: I don't understand how you get the maps. For this you need the marginal distribution of rainfall at every pixel. How do you get this?

Response: We get the response surface for the marginal distribution parameters of rainfall at every pixel using a thin plate spline regression against longitude and latitude. We unintentionally omitted these details in the original version, but have included them in the updated manuscript.[7]

Minor comment #23:

l. 469: average spatial rainfall: I'm confused. How can you transform return levels to averages?

Response: We use areal reduction factors ARFs for this conversion and will clarify the text. ARFs a standard design method used to transform an intensity of extreme rainfall at a point to an average rainfall intensity over a spatial domain with an equivalent probability of exceedance (Ball et al., 2016; Myers, 1980; Omolayo, 1993; Shaw et al., 2011; Siriwardena and Weinmann, 1996).

References used for this response:

Ball, J. et al., 2016. Australian Rainfall and Runoff: A Guide to Flood Estimation. © Commonwealth of Australia (Geoscience Australia).

Myers, V.A., 1980. A methodology for point-to-area rainfall frequency ratios. In: Zehr, R.M. (Ed.), Dept. of Commerce, National Oceanic and Atmospheric Administration, National Weather Service. Silver Spring, Md.

Omolayo, A.S., 1993. On the transposition of areal reduction factors for rainfall frequency estimation. J. Hydrol. 145 (1), 191–205. https://doi.org/10.1016/0022-1694(93) 90227-Z.

Shaw, S.B., Royem, A.A., Riha, S.J., 2011. The relationship between extreme hourly precipitation and surface temperature in different hydroclimatic regions of the United States. J. Hydrometeorol. 12 (2), 319–325. https://doi.org/10.1175/2011jhm1364.1.

Siriwardena, L., Weinmann, P., 1996. Derivation of areal reduction factors for design rainfalls in Victoria for Rainfall Durations 18–120 hours. Report, 96(4): 60.

Minor comment #24:

Fig. 11 at the river crossing: which crossing are you talking about? There are several.

Response: Thanks, we have clarified it in the updated manuscript.

Minor comment #25:

[7] Line 438: "In order to obtain the maps in Fig. 7 and Fig. 8, a thin plate spline regression against longitude and latitude was employed to build the response surface for the marginal distribution parameters of rainfall at every pixel."

l. 495-497: Although Fig 11 … not part of the method → I don't understand these two sentences. What do you mean by "this is not a physical timing difference"?

Response: This text means that our method focuses on the peak of the conditional design hydrograph and does not consider the difference in the timing of the peak. We have improved the explanation to clarify this.[8]

Minor comment #26:

Fig. 12: I don't understand the AEP. Wouldn't it be clearer with return periods instead of AEP?

Response: As with major comment #6, we consider that AEP is a confused term for the conditional probability in Fig. 12. We have removed this figure and associated discussion.

Minor comment #27:

l. 511: extreme rainfall intensity → over a catchment?

Response: Thanks, we have fixed this.

Minor comment #28:

l. 520: and → as a function of?

Response: Thanks, we have fixed this.

Minor comment #29:

Fig. 13: as for Fig. 12, would be clearer to show return periods in the x-axis?

Response: Unlike minor comment #26 focussed on Fig. 12, we think the term "annual exceedance probability" (AEP) is straightforward when applied to the joint probability shown in Fig. 13. The AEP and return period are interchangeable as an inverse relationship, but we expect some readers are more familiar with the terminology of return periods. We have audited our use of these terms throughout the manuscript and will apply a consistent terminology.

Minor comment #30:

Caption of Fig. 13: please explain what are the green segments

---

[8] Line 494: "Although Fig. 9 shows a difference in terms of the time taken to reach the peak flows, the two design hydrographs are separate and this is not a physical timing difference."

Response: The green segments are to indicate the interpolation of the individual element failure probability to a system failure probability (discussion line 530). We have added this detail to the figure caption so the description is self contained.[9]

Minor comment #31:

l. 529: 1% annual exceedance prob → 1% AEP

Response: Thank you. We have fixed this.

Minor comment #32:

l. 573: 1.74 → I guess this number depends on the considered levels

Response: Yes, this number depends on the pair of locations that we analyse the conditional probability as well as the considered levels, so we have added a clarification of the considered levels in the revised version of the manuscript.[10]

Minor comment #33:

l. 611: inverted max-stable → inverted max-stable process

Response: Thank you, we will fix it when revising the manuscript.

Minor comment #34:

Fig. S1: I don't understand the figure. Could you please explain what a given point represents? Given Table 1, I would have expected to have points at A=91, 294, 341, 771, 1020, which is not the case.

Response: Fig. S1 provides relationships between areal reduction factors (ARFs) and area (in km^2) for different return periods for the case study catchments. These relationships are calculated through the simulation of inverted Brown-Resnick process over equally sized grid points. To get the ARFs for each of subcatchments in the case study (corresponding to area A=*91, 294, 341, 771, 1020*), we need to interpolate these relationships. We will improve the explanation in the revised version of the manuscript.

---

[9] Line 527: "The green lines help to interpolate the individual element failure probability from a given system failure probability of 1%. Both horizontal axis and vertical axis are constructed at a double log scale for viewing purposes."

[10] Line 567: "for the two catchments having the strongest dependence (Fig. 7). The corresponding conditional flows were then estimated using a hydrological model WBNM and shown to be strongly related to the ratio of conditional and unconditional rainfall extremes (Fig. 9)."

Response to the Reviewer #3

In general, the paper is well written. However, I have some concerns regarding the real contribution (novelty), connection with the literature and in particular with copula studies, as well as comparison with other models. Main comments:

Response: Thank you for your comments. We respond in detail below (your comments in italic font and our responses in normal font).

Major comment #1:

1. Some important papers related to the topic are missing and more importantly the comparison with them not only in terms of results but also in terms of advantages and drawbacks (e.g. Bardossy and Pegram, 2009, Durocher et al. 2016 and Requena et al. 2018).

Response: Thank you for the suggestion. We have added discussion on these paper to the revised manuscript.[11]

Major comment #2:

2. Regarding the issues motivating the study: the first one seems to be already fixed by Le et al. 2018b (as indicated on page 5), and the second issue is not clear (seems to be written as a statement not as an issue).

Response: Thank you for pointing this out. The second issue relates to the spatial properties of asymptotic dependence (explored in Le et al., 2018a). While these two issues have been separately addressed in previous papers, the contribution is to show how to combine the methods to solve a realistic design problem.

References used for this response:

Le, P. D., Davison, A. C., Engelke, S., Leonard, M., and Westra, S.: Dependence properties of spatial rainfall extremes and areal reduction factors, Journal of Hydrology, Submitted, 2018a.

Le, P. D., Leonard, M., and Westra, S.: Modeling Spatial Dependence of Rainfall Extremes Across Multiple Durations, Water Resources Research, 54, 2233-2248, 2018b.

[11] Line 59: "Most rainfall models operate at the daily timescale (Bárdossy and Pegram, 2009; Baxevani and Lennartsson, 2015; Bennett et al., 2016b; Hegnauer et al., 2014; Kleiber et al., 2012; Rasmussen, 2013), whereas many catchments respond at subdaily timescales."
Line 47: "Several frameworks have been demonstrated based directly on streamflow observations, including functional regression (Requena et al., 2018), multisite copulas (Renard and Lang, 2007), and spatial copulas (Durocher et al., 2016)."

Major comment #3:

3. The topic can also be closely related to regional frequency analysis or estimation at ungauged basins. The authors did not make this connection or show the difference. In the first case (similarity or connection), a huge literature exists and should be considered.

Response: Thanks for your comment. We have discussed differences to regional frequency analysis and methods of estimation in the revised manuscript.[12]

[12] Line 72: "Regional frequency analysis is one type of method to estimate IDF curves, where the precision of at-site estimates is improved by pooling data from sites in the surrounding region (Hosking and Wallis, 1997). These methods can be combined with spatial interpolation methods to estimate parameters for any ungauged location of interest (Carreau et al., 2013). To determine an effective mean depth of rainfall over a catchment with the same exceedance probability as at a gauge location, the pointwise estimate of extreme rainfall is multiplied by an areal reduction factor (ARF) (Ball et al., 2016). However, such methods do not account for information on the spatial dependence of extreme rainfall—whether for single storm duration, or for the more complex case of different durations across a region (Bernard, 1932; Koutsoyiannis et al., 1998). The lack of dependence prevents these approaches from being applied to estimate conditional or joint flood risk at multiple points in a catchment or across several catchments, as would be required for a civil infrastructure system."

Major comment #4:

4. The paper focused on a case study (a given set of data). However, the effect of some factors on the performance of the model as not discussed and not studied: for instance, and not limited to, the dimensionality (number of sites) and the size of the subgroups.

Response:

Thanks for your comment. This is beyond the scope of the current study.

Major comment #5:

5. An important missing element from the paper is the notion of copulas which is the most important when dealing with dependence. There is a huge literature in both hydrology and statistics (even in spatial dependence). I'm surprised to not see it in the paper.

Response: We have added literature on copulas into the revised manuscript.[13]

Major comment #6:

6. In section 4: why the GPD is used directly without model selection procedure? Why it is the same for all sites? The GPD is usually asymptotically justified which is not enough (and less justified in hydrology because of the sample sizes) and does not depend on the data at hand. It should be considered as a distribution among others (like GEV for block extremes).

Response: Thank you for this comment. We used the GPD because, in contrast to block maxima, it allows us to consider concurrent rainfall extremes and therefore enables the study of dependence. The intention in this paper is not to work through repetitive fitting of different distributions, but to demonstrate a plausible method based on joint rainfall extremes for the design of linear infrastructure. The same distribution is used at each site with variation at each site carried by the parameters. The marginal model adopted is not perfect, but it is plausible, and sufficient for the intent of showing the application of rainfall dependence to design.

Major comment #7:

7. Lines 245-248: please provide other alternative models and justify the choice of your model.

Response: Thank you. We have added justification of the choice of the Brown-Resnick model in the revised manuscript. For example, Le et al. (2018a) show it has better performance than the extremal-t model.[14]

---

[13] Line 91: "Copulas including the extremal-t copula (Demarta and McNeil, 2005), and the Husler-Reiss copula (Hüsler and Reiss, 1989) have also been used to model rainfall dependence."

[14] Line 253: "From Eq. (2), different models for W give different inverted max-stable processes. There are two popular and easily-simulated classes of model for the inverted max-stable processes: the Brown-Resnick model (Asadi et al., 2015; Huser and Davison, 2013; Kabluchko et al., 2009; Oesting et al., 2017), and extremal-t model (Opitz, 2013). This study uses the Brown-Resnick form of equations from the family of an inverted max-stable process because Le et al. (2018a) showed it has better performance than the extremal-t model."

Le, P. D., Davison, A. C., Engelke, S., Leonard, M., and Westra, S.: Dependence properties of spatial rainfall extremes and areal reduction factors, Journal of Hydrology, Submitted, 2018a.

Major comment #8:

8. The assumption, on page 11 line 215, is it reasonable? Is it verified in your case study?

Response: Thank you very much. The assumption of AEP neutrality in rainfall-runoff design is a standard assumption when using IDF curves. While the assumption is in widespread use, it is not without limitation as this issue was explored in to the following two papers.

Bennett, B., Leonard, M., Deng, Y., & Westra, S. (2018). An empirical investigation into the effect of antecedent precipitation on flood volume. Journal of Hydrology, 567, 435-445.

Rahman, A., Weinmann, P. E., Hoang, T. M. T., & Laurenson, E. M. (2002). Monte Carlo simulation of flood frequency curves from rainfall. Journal of Hydrology, 256(3-4), 196-210.

Major comment #9:

9. How the hydrological model (ex. WBNM) is integrated in the steps of fig 4?

Response: The hydrological model (i.e. WBNM) is used to transform the conditional rainfall to conditional flow. A label has been added in the revised version of the manuscript to show this (on the arrow between the see the squares for Section 4.5 and Section 4.6 in the top-right of Figure 4).

Minor comment #1:

1. Fig 4: Why in the independent model, no fitting is required? What it means?

Response: Thank you for pointing this out. The term "the independent model" here is not clear. We have changed it to "the case of independence" and have clarified that we mean the case where rainfall extremes occur independently in space.

Minor comment #2:

2. Sentence from lines 237-240 is long and not clear. Please consider reformulating.

Response: Thank you. We have reworded these sentences in the revised manuscript.[15]

---

[15] Line 232: "Without loss of generality it can be assumed that the margins of Z have a unit Fréchet distribution. An important property of dependence in the extremes is whether or not two variables are likely/unlikely to co-occur as the extremes become rarer, as this can significantly influence the estimate of frequency for flood events of large magnitude."

Minor comment #3:

3. Page 13: this text requires to be more accurate about the terms and notation.

Response: Thank you very much. We have clarified this text in the revised manuscript.

Minor comment #4:

4. Lines 287-290: is this case not covered by equation 4?

Response: Thank you. We will rewrite this comment on equation 4. We have clarified that the equation can be used for both cases.

Minor comment #5:

5. All text in page 16 and part of page 17 seems trivial and does not worth all this space. Other more important information deserve this space.

Response: We have removed this material, which will create significantly more space.

Minor comment #6:

6. It is not clear in section 4.6 if the authors consider one hydrological model (WBNM) or other models (see for instance lines 376 and 384).

Response: Thank you for your comment. There is only one type of model (WBNM), but different configurations for each catchment. We have clarified this in the revised text.[16]

Minor comment #7:

7. Line 408 : how you can say the model has reasonable fit? Based on what? And compared to what?

Response: Thank you. We have more explicitly indicated that the comment on fitting relates to Figure 8 (Figure 6 in the updated version). We have also emphasized that the main feature of the model shown in these figures is the relationship at h=0, for the case of dependence between two different durations at the same location.[17]

Minor comment #8:

8. Line 538 : I'm not sure about this statement. It is not true in many situations.

---

[16] Line 385: "Hydrological models (WBNM) for the case study area were developed and calibrated (WMAWater, 2011)."

[17] Line 411: "Figure 6 indicates that the model has a reasonable fit to the observed data given the small number of dependence parameters. Although the theoretical coefficient (red line) does not perfectly at long distances, the main interest is in short distances, especially at $h = 0$ for the case of dependence between two different durations at the same location."

Response: Thank you for your comment. We have restricted our commentary to conventional hydrological design that is based on IDF curves, which is more defensible than the original comment which was too general. By construction IDF curves are focused are point-wise estimators of extremes, thus a given design is focused on independent application of univariate statistics.

Spatially dependent Intensity-Duration-Frequency curves to support the design of civil infrastructure systems

Phuong Dong Le[1,2], Michael Leonard[1], Seth Westra[1]

[1]*School of Civil, Environmental and Mining Engineering, University of Adelaide, Adelaide, South Australia, Australia*

[2]*Thuyloi University, Hanoi, Vietnam*

~~*Email: phuongdong.le@adelaide.edu.au*~~

Email: lephuongdong_tb@tlu.edu.vn

Keywords: areal reduction factor, asymptotic independence, conditional probability, duration dependence, extreme rainfall, flood probability, inverted max-stable process, joint probability, spatially dependent Intensity-Duration-Frequency,

Abstract

Conventional flood risk methods typically focus on estimation at a single location, which is inadequate for civil infrastructure systems such as road or railway infrastructure. This is because rainfall extremes are spatially dependent, so that to understand overall system risk it is necessary to assess the interconnected elements of the system jointly. For example, when designing evacuation routes it is necessary to understand the risk of one part of the system failing given that another region is flooded or exceeds the level at which evacuation becomes necessary. Similarly, failure of any single part of a road section (e.g., a flooded river crossing) may lead to the wider system's failure (i.e. the entire road becomes inoperable). This study demonstrates a spatially dependent Intensity-Duration-Frequency curve framework that can be used to estimate flood risk across multiple catchments, accounting for dependence both in space and across different critical storm durations. The framework is demonstrated via a case study of a highway upgrade, comprising five bridge crossings where the upstream contributing catchments each have different times of concentration. The results show that conditional and unconditional design flows can differ by a factor of two, highlighting the importance of taking an integrated approach. There is also a reduction in the failure probability of the overall system compared with the case of no spatial dependence between storms. The results demonstrate the

potential uses of spatially dependent Intensity-Duration-Frequency curves and suggest the need for more conservative design estimates to take into account conditional risks.

1. Introduction

Methods for quantifying the flood risk of civil infrastructure systems such as road and rail networks require considerably more information compared to traditional methods that focus on flood risk at a point. For example, the design of evacuation routes requires the quantification of the risk that one part of the system will fail at the same time that another region is flooded or exceeds the level at which evacuation becomes necessary. Similarly, a railway route may become impassable if any of a number of bridges are submerged, such that the 'failure probability' of that route becomes some aggregation of the failure probabilities of each individual section. Successful estimation of flood risk in these systems therefore requires recognition both of the networked nature of the civil infrastructure system across a spatial domain, as well as the spatial and temporal structure of flood-producing mechanisms (e.g. ~~storms and extreme rainfall) that can lead to system failure (e.g., Leonard et al. (2014)~~storms and extreme rainfall) that can lead to system failure (e.g., Leonard et al. (2014), ~~Seneviratne et al. (2012)~~Seneviratne et al. (2012), ~~Zscheischler et al. (2018)~~Zscheischler et al. (2018)).

One way to estimate such flood probabilities is to directly use information contained in historical streamflow data. For example, annual maximum streamflow at two locations might be assumed to follow a bivariate generalized extreme value distribution ~~(Favre et al., 2004; Wang, 2001; Wang et al., 2009)~~(Favre et al., 2004; Wang, 2001; Wang et al., 2009)~~, which can then be used to estimate both conditional probabilities (e.g. the probability that one river is flooded given that the other river level exceeds a specified threshold) and joint probabilities (e.g. the probability that one or both rivers are flooded). However, continuous streamflow data are often not available at the locations most relevant to the civil infrastructure system in question, or the catchment conditions have changed to a degree that reflects historical streamflow records as unrepresentative of likely future risk. Thus, direct application of streamflow data for flood risk quantification in civil infrastructure systems does not represent a viable approach for the majority of situations.~~, which can then be used to estimate both conditional probabilities (e.g. the probability that one river is flooded given that the other river level exceeds a specified threshold) and joint probabilities (e.g. the probability that one or both rivers are flooded). Several frameworks have been demonstrated based directly on streamflow observations, including functional regression (Requena et al., 2018), multisite copulas (Renard and Lang, 2007), and spatial copulas (Durocher et al., 2016). However, this paper focuses on rainfall-based methods, as in many instances continuous streamflow data are unavailable or insufficient at the locations of interest, or the catchment conditions have changed such that historical streamflow records as unrepresentative of likely future risk.

To ~~deal with these difficulties, two alternative~~overcome common limitations of streamflow data, rainfall-based approaches are commonly used. ~~The first~~One method uses continuous rainfall data (either historical or generated) to compute continuous streamflow data using a rainfall-runoff model ~~(Boughton and Droop, 2003; Cameron et al., 1999; He et al., 2011; Hegnauer et al., 2014; Pathiraja et al., 2012),~~(Boughton and Droop, 2003; Cameron et al., 1999; He et al., 2011; Hegnauer et al., 2014; Pathiraja et al., 2012), with flood risk then estimated based on the simulated streamflow time series. This method is computationally intensive and given the challenge of reproducing a wide variety of statistics across many scales, can have difficulties in modelling the dependence of extremes. Most rainfall models operate at the daily timescale ~~(Baxevani and Lennartsson, 2015; Bennett et al., 2016b; Hegnauer et al., 2014; Kleiber et al., 2012; Rasmussen, 2013),~~(Bárdossy and Pegram, 2009; Baxevani and Lennartsson, 2015; Bennett et al., 2016b; Hegnauer et al., 2014; Kleiber et al., 2012; Rasmussen, 2013), whereas many catchments respond at subdaily timescales. The capacity of space-time rainfall models to simulate the statistics of sub-daily rainfall remains a challenging research problem ~~(Leonard et al., 2008).~~(Leonard et al., 2008). One approach is to exploit the relative abundance of data at the daily scale, then apply a downscaling model to reach subdaily scales ~~(Gupta and Tarboton, 2016).~~(Gupta and Tarboton, 2016). Continuous simulation is receiving ongoing attention and increasing application, yet there remain limitations when applying these models in many practical contexts.

~~The~~A second rainfall-based approach proceeds by ~~conducting the~~applying probability calculations on rainfall, to construct ‘Intensity-Duration-Frequency’ (IDF) curves, which are then translated to a runoff event of equivalent probability via either empirical models such as the ~~Rational~~rational method to estimate peak flow rate ~~(Kuichling, 1889; Mulvaney, 1851)~~(Kuichling, 1889; Mulvaney, 1851) ~~to~~

~~estimate peak flow rate,~~, or via event-based rainfall-runoff models that are able to simulate the full flood hydrograph ~~(Boyd et al., 1996; Chow et al., 1988; Laurenson and Mein, 1997)~~(Boyd et al., 1996; Chow et al., 1988; Laurenson and Mein, 1997)~~. Currently IDF curves are estimated either at a point location, or are estimated over a spatial domain by multiplication with an areal reduction factor (ARF) to convert point rainfall to spatially averaged rainfall of an equivalent exceedance probability (Ball et al., 2016); this information then can be used to estimate either peak flow or the flood hydrograph at any point location within a catchment. However, such methods do not account for information on the spatial dependence of extreme rainfall – whether for single storm duration across a region, or for the more complex case of different durations across a region (Bernard, 1932; Koutsoyiannis et al., 1998). This prevents these approaches from being applied to estimate conditional or joint flood risk at multiple points in a catchment or across several catchments as would be required for a civil infrastructure system.~~

~~Although tailored multivariate approaches can be applied to estimate conditional and joint probabilities of extreme rainfall for specific situations (e.g., Kao and Govindaraju (2008), Wang et al. (2010), Zhang and Singh (2007)), the development of a unified methodology that integrates with existing IDF-based flood estimation approaches remains elusive. This is particularly challenging given that it is not only necessary to preserve dependence of rainfall across space, but also to account for dependence across storm burst durations, as different parts of the system may be vulnerable to different critical duration storm events. To this end, arguably the most promising recent research direction has been the application of max-stable process theory that is able to represent storm-level dependence (de Haan, 1984; Schlather, 2002). This has been applied on a spatial domain by Padoan et al. (2010), who calculated conditional probabilities for a spatial domain located in United States. However, to ensure that this general approach can be applied for practical flood estimation problems, two further problems need to be overcome:~~

1. ~~The approach needs to not only account for spatial dependence for rainfall 'events' of a single duration (e.g. the field of annual maximum daily rainfall data), but must also account for dependence across multiple durations. This was addressed by Le et al. (2018b), who linked~~

~~the max-stable model of Brown and Resnick (1977) and Kabluchko et al. (2009) with the duration-dependent model of Koutsoyiannis et al. (1998), in order to create a model that could be used to reflect dependencies between nearby catchments of different sizes.~~

2. ~~Given that often the interest is in rare flood events, the model needs to capture appropriate asymptotic properties of spatial dependence as the events become increasingly extreme. Recent evidence is emerging that rainfall has an asymptotically independent characteristic (Le et al., 2018a; Thibaud et al., 2013), which means that the level of the rainfall's dependence reduces with an increasing return period (Wadsworth and Tawn, 2012). This implies that inverted max-stable models, which are asymptotically independent, are likely to be preferable as an approach for representing spatially dependent IDF information. An added benefit of correctly representing asymptotic dependence is that information on areal reduction factors can be obtained directly from the model, rather than estimating ARF information independently from the computation of the IDF curves.~~

~~This study addresses both these issues by demonstrating the application of the inverted max-stable process to estimate joint and conditional probabilities of flood-producing rainfall in the form of spatially dependent IDF curves. This approach adapts the methods developed by (Le et al., 2018b) to inverted max-stable models, and then uses the derived spatially dependent IDF curves combined with the extracted information on AFRs as the basis for transforming the rainfall into flood flows.~~. Regional frequency analysis is one type of method to estimate IDF curves, where the precision of at-site estimates is improved by pooling data from sites in the surrounding region (Hosking and Wallis, 1997). These methods can be combined with spatial interpolation methods to estimate parameters for any ungauged location of interest (Carreau et al., 2013). To determine an effective mean depth of rainfall over a catchment with the same exceedance probability as at a gauge location, the pointwise estimate of extreme rainfall is multiplied by an areal reduction factor (ARF) (Ball et al., 2016). However, such methods do not account for information on the spatial dependence of extreme rainfall—whether for single storm duration, or for the more complex case of different durations across a region (Bernard, 1932; Koutsoyiannis et al., 1998). The lack of dependence prevents these approaches from being applied to estimate conditional or joint flood risk at multiple points in a catchment or across several catchments, as would be required for a civil infrastructure system.

Although multivariate approaches can be tailored to estimate conditional and joint probabilities of extreme rainfall for specific situations (e.g., Kao and Govindaraju (2008), Wang et al. (2010), Zhang and Singh (2007)), the development of a unified methodology that integrates with existing IDF-based flood estimation approaches remains elusive. This is particularly challenging given that it is not only necessary to preserve dependence of rainfall across space, but also to account for dependence across storm burst durations, as different parts of the system may be vulnerable to different critical duration storm events. To this end, max-stable process theory has been demonstrated to represent storm-level dependence (de Haan, 1984; Schlather, 2002) and used to calculate conditional probabilities for a spatial domain (Padoan et al., 2010). Copulas including the extremal-t copula (Demarta and McNeil, 2005), and the Husler-Reiss copula (Hüsler and Reiss, 1989) have also been used to model rainfall dependence.

This study applies a max-stable approach with an emphasis on practical flood estimation problems:

1. The approach needs to account for, not only the spatial dependence of rainfall ‘events’ of a single duration, but also the dependence across multiple durations. This was addressed by Le et al. (2018b), who linked the max-stable model of Brown and Resnick (1977) with the duration-dependent model of Koutsoyiannis et al. (1998), to create a model that could be used to reflect dependencies between nearby catchments of different sizes.
2. Given that often the interest is in rare flood events, the model needs to capture appropriate asymptotic properties of spatial dependence as the events become increasingly extreme. Recent evidence is emerging that rainfall has an asymptotically independent characteristic (Le et al., 2018a; Thibaud et al., 2013), which means that the level of the rainfall’s dependence reduces with an increasing return period (Wadsworth and Tawn, 2012). The requirement of asymptotic independence indicates that inverted max-stable models are preferable over max-stable models.

This study adapts the methods developed by Le et al. (2018b) to inverted max-stable models to derive spatially-dependent IDF curves and ARFs as the basis for transforming rainfall into flood flows. The approach is demonstrated on a highway system spanning 20 km with five separate bridge crossings, and with the contributing catchment at each crossing having a different time of concentration.

The case study is designed to address two related questions: (i) "What flood flow needs to be used to design a bridge that will fail only once on average every M times (e.g., $M = 10$ for a 10-year event) that a neighbouring catchment is flooded?"; and (ii) "What is the probability that the overall system fails given that each bridge is designed to a specific exceedance probability event (e.g., the 1% annual exceedance probability event)?" The method for resolving these questions represents a new paradigm in which to estimate flood risk for engineering design, by focusing attention on the risk of the entire system, rather than the risk of individual system elements in isolation.

In the remainder of the paper, Section 2 emphasises the need for spatially dependent IDF curves in flood risk design, followed by Section 3 which outlines the case study and data used. Section 4 explains the methodology of the framework, including a method for analysing the spatial dependence of extreme rainfall across different durations. It also includes an algorithm with which to use that information in estimating the conditional and joint probabilities of floods. The results, and a discussion on the behaviour of flood due to the spatial and duration dependence of rainfall extremes, are provided in Section 5. Conclusions and recommendations follow in Section 6.

2. The need for spatially dependent IDF curves in flood risk estimation

The main limitation of conventional methods of flood risk estimation is that they isolate bursts of rainfall and break the dependence structure of extreme rainfall. Figure 1 demonstrates a traditional process of estimating at-site extreme rainfall for two locations (gauge 1, gauge 2) and three durations (1, 3, and 5 hr) ~~(Stedinger et al., 1993)~~(Stedinger et al., 1993). The process first involves extracting the extreme burst of rainfall for each site, duration and year from the continuous rainfall data, and then fitting a probability distribution (such as the Generalised Extreme Value (GEV) distribution) to the extracted data. Figure 1 demonstrates that, through the process of converting the continuous rainfall data to a series of discrete rainfall 'bursts', this process breaks both the dependence with respect to duration and space. Firstly, the duration dependence is broken by extracting each duration separately, whereas for the hypothetical storm in Fig. 1 it is clear that the annual maxima from some of the extreme bursts come from the same storm. Secondly, the spatial dependence is broken because each site is analysed independently. Again, for the hypothetical storm of Fig. 1 it can be seen that the 5 hr storm has occurred at the same time across the two catchments, and this information is lost in the subsequent probability distribution curves. Lastly, there is cross-dependence in space and duration. For example, the 1 hr extreme from gauge 2 occurs at the same time as the 5 hr extreme from gauge 1. This may be relevant if there are two catchments with times of concentration matching 1 hr and 5 hr respectively, where catchments are neighbouring or nested.

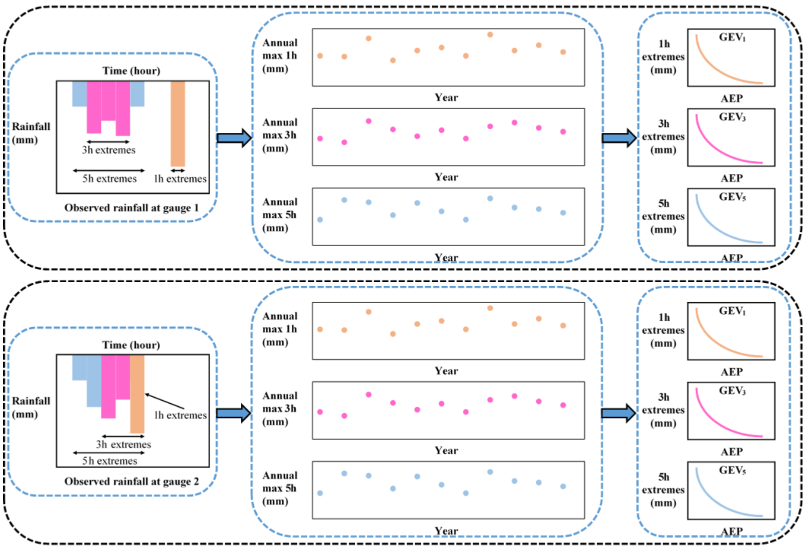

Figure 1. Illustration of process to estimate rainfall extremes for each individual location in conventional flood risk approach, the upper panel is for gauge 1 and the lower panel is for gauge 2.

Having obtained the IDF curves for individual locations in Fig. 1, the next step is commonly to convert this to spatial IDF maps by interpolating results between gauged locations. Figure 2 shows hypothetical IDF curves from individual sites, with a separate spatial contour map usually provided for each storm burst duration. In a conventional application the respective maps are used to estimate the magnitude of extreme rainfall over catchments for a specified time of concentration. The IDF curves are combined with an areal reduction factor (ARF) to determine the volume of rainfall over a region (since rainfall is not simultaneously extreme at all locations over the region). However, because the spatial dependence was broken in the analysis of IDF curves, the ARF come from a separate analysis and are an attempt to correct for the broken spatial relationship within a catchment ~~(Bennett et al., 2016a)~~(Bennett et al., 2016a). Lastly, the rainfall volume over the catchment is combined with a temporal pattern and input to a runoff model to simulate flood-flow at a catchment's outlet. Where catchment flows can be considered independently this process has been acceptable for conventional design, but because this process does not account for dependence across durations and across a region, it is not possible to address problems that span multiple catchments, as with civil infrastructure systems.

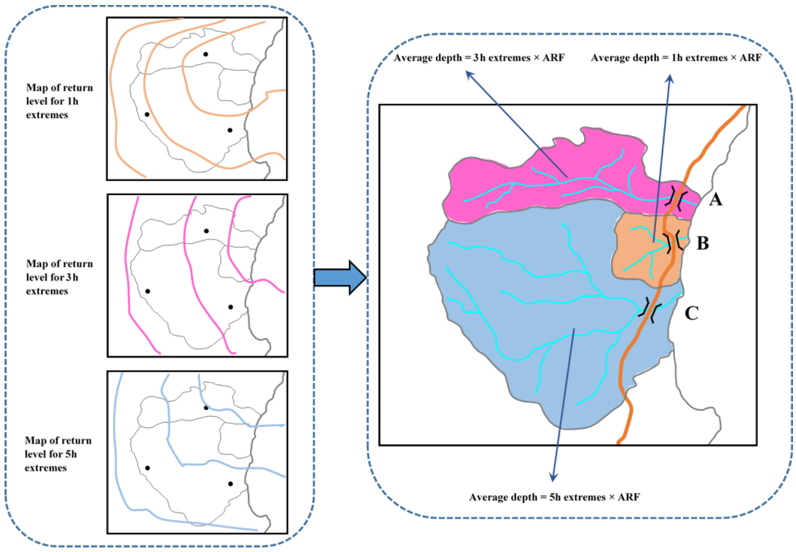

Figure 2. Illustration of map of return level and how to use it in estimating flood flow in conventional flood risk estimates approach.

The process in Fig. 1 breaks out the dependence of the observed rainfall, which makes the conventional approach unable to analyse the dependence of flooding at two or more separate locations. Instead, this paper advocates for spatially dependent IDF curves which are developed by retaining the dependence of observed rainfall in the estimation of extremal rainfall. By applying spatially dependent IDF curves to a rainfall-runoff model, the dependence of flooding between separate locations can be achieved.

3. Case study and data

The region chosen for the case study is in the mid north coast region of New South Wales, Australia. This region has been the focus of a highway upgrade project and has an annual average daily traffic volume on the order of 15,000 vehicles along the existing highway. The upgrade traverses a series of coastal foothills and floodplains for a total length of approximately 20 km. The project's major river crossings consist of extensive floodplains with some marsh areas.

The case study has five main catchments that are numbered in sequence in Fig. 3: (1) Bellinger, (2) Kalang River, (3) Deep Creek, (4) Nambucca and (5) Warrell Creek. The area and time of concentration of these catchments is summarised in Table 1, with the latter estimated using the ratio of the flow path length and average flow velocity ~~(SKM, 2011)~~(SKM, 2011). The Deep Creek catchment has a time of concentration of 8.3 hr, while the other four catchments have much longer times of concentration, ranging from 27.8 to 38.9 hr. These require the estimates of spatial dependence across different durations of rainfall extremes. Although the spatial dependence across rainfall durations would be expected to be lower than across a single duration, since short- and long-rain events are often driven by different meteorological mechanisms ~~(Zheng et al., 2015)~~(Zheng et al., 2015), it is nonetheless likely that some level of spatial dependence would exist and need to be integrated into the risk calculations. This is particularly of relevance given extremal rainfall in this region is strongly associated with 'east coast low' systems off the eastern coastline, whereby extreme hourly rainfall bursts are often embedded in heavy multi-day rainfall events.

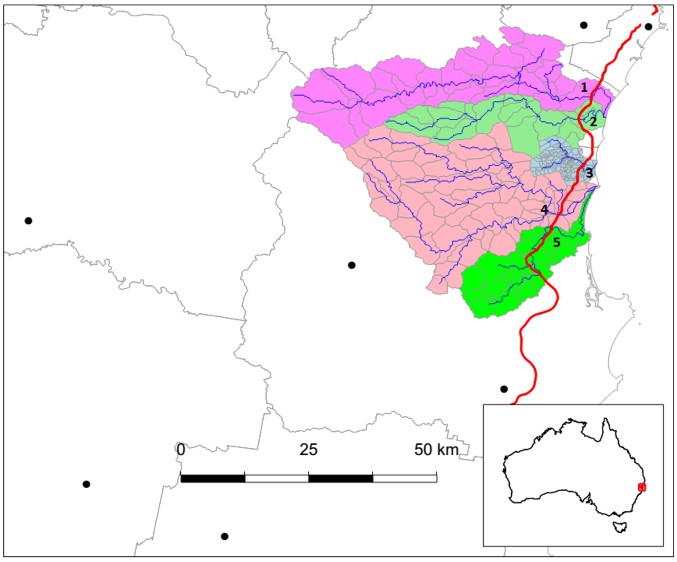

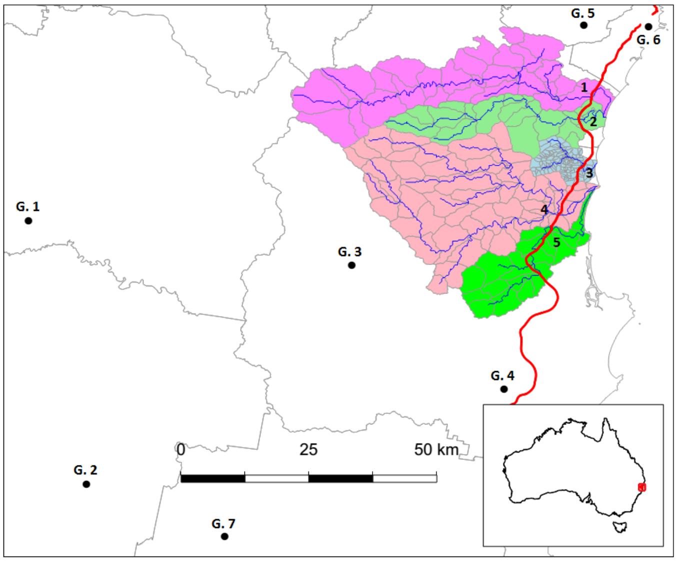

Figure 3. Map of the case study in New South Wales, Australia. The black dots indicate the rainfall gauges~~,~~ (G. 1 to G. 7), the red line indicates the Pacific Highway upgrade project, and the blue lines indicate the main river network. The numbers from one to five indicate the locations of the main river crossings.

Table 1. Summary of properties for catchments in the case study.

No.	**Catchment**	**Area**	**Raw time of concentration**

		(ha)	(hour)
1	Bellinger	77150	37
2	Kalang River	34140	33
3	Deep Creek	9180	8
4	Nambucca (upper)	102015	38
5	Warrell Creek	29440	27

The black circles in Fig. 3 represent the sub-daily rain stations used for this study. There were 7 sub-daily stations selected, with 35 years of record in common for the whole region. The data was available at a 5 minute interval and aggregated to longer durations. For convenience in comparing the times of concentration between the catchments, this study assumes a time of concentration of 9 hr for the Deep Creek catchment, while identical times of concentration of 36 hr are assumed for the other four catchments.

4. Methodology

This section provides the method used to estimate the conditional and joint probabilities of flood for civil infrastructure systems based on rainfall extremes, which is explained according to the steps shown in Fig. 4. First, the generalized Pareto distribution (GPD) is used as marginal distribution to fit to observed rainfall for all duration at each locations (Section 4.1). After that, an inverted max-stable process is introduced and then fitted to rainfall extremes of identical or different durations (Sections 4.2 & 4.3). The conditional and joint probabilities of rainfall are then estimated in Section 4.4, which is followed by the simulation to calculate areal reduction factor (ARF) in Section 4.5. An event-based rainfall-runoff model is employed in Section 4.6 to transform conditional rainfall to conditional flows. With an assumption ~~of~~that there is a one-to-one correspondence between rainfall intensity and flow rate, the joint flood probability for the case study is equal to the joint probability of rainfall. An analysis for the independent model (the case of complete independence) is also implemented for comparison.

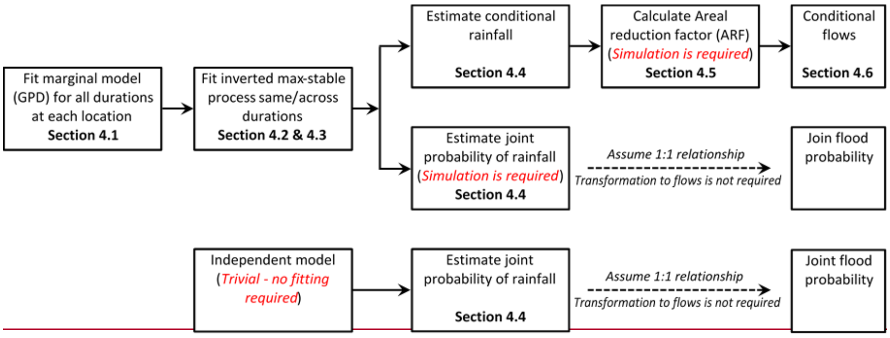

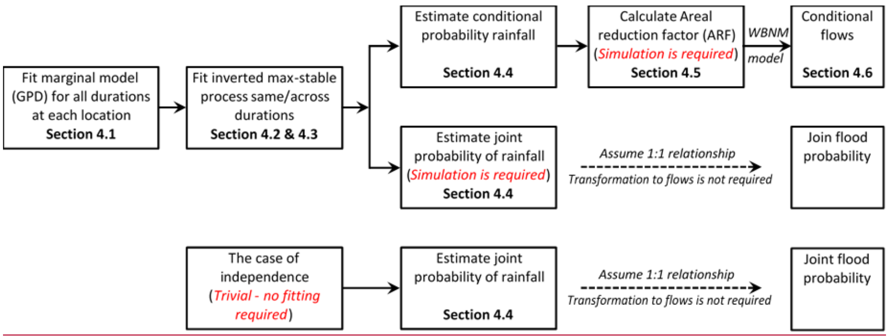

Figure 4. The flow chart for the overall methodology.

4.1. Marginal model for rainfall

This study defines extremes as those greater than some threshold u. For large u, the distribution of Y conditional on $Y > u$ may be approximated by the generalized Pareto distribution (GPD) ~~(Davison and Smith, 1990; Pickands, 1975; Thibaud et al., 2013)~~(Pickands, 1975; Davison and Smith, 1990; Thibaud et al., 2013):

$$G(y) = 1 - \left\{1 + \frac{\xi(y-u)}{\sigma_u}\right\}^{-1/\xi}, \quad y > u, \tag{1}$$

defined on $\{y: 1 + \xi(y-u)/\sigma_u > 0\}$ where $\sigma_u > 0$ and $-\infty < \xi < +\infty$ are scale and shape parameters, respectively. The probability that a level y is exceeded is then $\Phi_u\{1 - G(y)\}$, where $\Phi_u = \Pr(Y > u)$.

The selection of the appropriate threshold u involves a trade-off between bias and variance. A threshold that is too low leads to bias because the GPD approximation is poor. A threshold too high leads to high variance because of a small number of excesses. Two diagnostic tests are used to determine the appropriate threshold u: the mean residual life plot and the parameter estimate plot ~~(Coles, 2001; Davison and Smith, 1990)~~(Coles, 2001; Davison and Smith, 1990). These methods use the stability property of a GPD, so that if a GPD is valid for all excesses above u, then excesses of a threshold greater than u should also follow a GPD. Detailed guidance of these methods can be found in Coles (2001).

Field Code Changed

Formatted: Underline, Font color: Hyperlink

4.2. Dependence model for spatial rainfall

Consider rainfall as a stationary stochastic process Z_i associated with a location x_i in a region of interest~~. Models~~ (the notation for ~~spatial extremes often use the convention~~the stochastic process is simplified from $Z(x_i)$ to Z_i). Without loss of ~~transforming marginal values to~~ generality it can be assumed that the margins of Z have a unit Fréchet distribution. An important property of dependence in the extremes is whether or not two variables are likely/unlikely to co-occur as the extremes become rarer, as this can significantly influence the estimate of frequency for flood events of large magnitude.

This is referred to as asymptotic dependence/independence, respectively. For the case of asymptotic independence, the dependence structure becomes weaker as the extremal threshold increases, which is formally defined as $\lim_{z\to\infty} P\{Z_1 > z|Z_2 > z\} = 0$ for all $x_1 \neq x_2$. The spatial extent of a rainfall event with asymptotically independent extremes will diminish as its rarity increases.

An example of an asymptotically independent model is the inverted max-stable process ~~(Wadsworth and Tawn, 2012)~~(Wadsworth and Tawn, 2012)~~. This study uses the Brown-Resnick form of equations from the family of an inverted max-stable process, and has been widely studied elsewhere (Asadi et al., 2015; Huser and Davison, 2013; Kabluchko et al., 2009; Oesting et al., 2017).~~. A general description of all continuous inverted max-stable processes that have standard exponential margins on a spatial domain X is

$$\tilde{\Omega}(x) = \min_{k\geq 1} U_k/W_k, \quad x \in X, \tag{2}$$

where U_k are points of a unit Poisson process on $(0, \infty)$ and the $W_k(x)$ are independent replicas of a continuous, non-negative stochastic process $W(x)$ in the spatial domain X, with $E\{W(x)\} = 1$ for all $x \in X$.

It is convenient to work with a simple inverted max-stable process with unit Fréchet margins, because the marginal distribution can easily be transformed back to the GPD scale. To transform the process $\tilde{\Omega}(x)$ to unit Fréchet margins, the following transformation is used:

$$\Omega(x) = -\frac{1}{\log\{1 - e^{-\tilde{\Omega}(x)}\}}, \quad x \in X, \tag{3}$$

then $\Omega(x)$ is an asymptotically independent process with unit Fréchet margins.

From Eq. (2), different models for W give different inverted max-stable processes. There are two popular and easily-simulated classes of model for the inverted max-stable processes: the Brown-Resnick model (Asadi et al., 2015; Huser and Davison, 2013; Kabluchko et al., 2009; Oesting et al., 2017), and extremal-t model (Opitz, 2013). This study uses the Brown-Resnick form of equations from the family of an inverted max-stable process because Le et al. (2018a) showed it has better performance than the extremal-t model.

4.3. Fitting the dependence model

One simple way to calibrate dependence models is to fit them to data by matching a suitable statistic. The dependence structure of the inverted max-stable process is represented by the pairwise residual tail dependence coefficient ~~(Ledford and Tawn, 1996)~~(Ledford and Tawn, 1996).

For a generic continuous process Z_i associated with a specific location x_i the empirical pairwise residual tail dependence coefficient η for each pair of locations (x_1, x_2) is

$$\eta(x_1, x_2) = \lim_{y \to \infty} \frac{\log P\{Z_2 > z\}}{\log P\{Z_1 > z, Z_2 > z\}}. \qquad (\cancel{2}4)$$

The value of $\eta \in (0,1]$ indicates the level of extremal dependence between Z_1 and Z_2 ~~(Coles et al., 1999)~~(Coles et al., 1999), with lower values indicating lower dependence. An example of how to calculate the residual tail dependence coefficient is provided in Appendix A for a sample dataset.

To estimate the dependence structure of an inverted max-stable model, the theoretical residual tail dependence coefficient function is usually fitted to its empirical counterpart. Here the residual tail dependence coefficient function is assumed to only depend on the Euclidean distance between two locations $h = \|x_1 - x_2\|$. The theoretical residual tail dependence coefficient function for the inverted Brown-Resnick model is given as:

$$\eta(h) = \frac{1}{2\Phi\left\{\sqrt{\frac{\gamma(h)}{2}}\right\}}, \qquad (\cancel{3}5)$$

where Φ is the standard normal cumulative distribution function, h is the distance between two locations, and $\gamma(h)$ belongs to the class of variograms $\gamma(h) = \|h\|^{\beta}/q$ for $q > 0$ and $\beta \in (0,2)$. The models are then fitted to the empirical residual tail dependence coefficients by modifying parameters q and β until the sum of squared errors is minimized.

In the case that extreme rainfall at locations x_1 and x_2 are of identical duration (i.e. both 36 hr), then the inverted max-stable process is fitted to the observations by minimizing the sum of the squared errors of the residual tail dependence coefficients. This information can be directly applied to the case where two catchments have a similar time of concentration owing to their similar shape and size.

However, there are many instances when two catchments of interest will have differing times of concentration; in particular, when the extreme rainfall at location x_1 and x_2 are of different durations (e.g., 36 hr and 9 hr), the dependence is less than the case of 36 hr and 36 hr. This observation is evident when considering the special case of a single location, i.e. the same point is considered twice, at a distance of $h = 0$. For the case where the duration is the same~~ where~~, the rainfall values are identical and have perfect dependence, but when the duration of extremes are different the values are not identical and the dependence is less. Therefore, an adjustment needs to be made to ensure that the theoretical pairwise residual tail dependence coefficient function suitably represents the observed pairwise residual tail dependence coefficients for the case of extreme rainfalls of different durations.

~~Following Le et al. (2018b),~~Following Le et al. (2018b), an adjusted approach is used by adding a nugget to the variograms as:

$$\gamma_{ad.}(h) = h^{\beta}/q + c(D - d)/d, \qquad (\cancel{4}6)$$

where h, β, and q are the same as those in Eq. (~~3~~5); d is the duration (in hours); $0 < d \leq D$, where D is the maximum duration of interest (e.g. $D = 36$ hr for the case study described in this paper); and c is a parameters to adjust dependence according to duration. This adjustment is intended to condition the behaviour of shorter duration extremes on a D-hour extreme of a specified magnitude. It is constructed to reflect the fact that when compared to a D-hour extreme, a shorter duration results in less extremal dependence. Cases involving conditioning of longer periods on shorter periods (such as a 36 hr extreme given a 9 hr extreme has occurred) ~~would require a different~~ can also use the relationship in Eq. (6), but with different parameter values.

To fit the inverted max-stable process for all pairs of durations at locations x_1 and x_2 (i.e. 36 hr and 12 hr, 36 hr and 9 hr, 36 hr and 6 hr, 36 hr and 2 hr, 36 hr and 1 hr), the theoretical pairwise residual tail dependence coefficient function in Eq. (~~3~~5) is used with the adjusted variogram from Eq. (~~4~~6) where the parameters β and q are first obtained from the fitted results of the case of identical 36 hr durations at location x_1 and x_2. The parameter c is obtained by a least square fit of the residual tail dependence coefficient across all durations.

4.4. Estimate of conditional and joint probabilities of rainfall extremes

The conditional probability $P\{Z_2 > z_2 | Z_1 > z_1\}$ is obtained from the bivariate inverted max-stable process cumulative distribution function (CDF) in unit Fréchet margins (Thibaud et al., 2013), which is given as:

$$P\{Z_1 \le z_1, Z_2 \le z_2\} = 1 - \exp\left\{-\frac{1}{g_1}\right\} - \exp\left\{-\frac{1}{g_2}\right\} + \exp[-V\{g_1, g_2\}], \qquad (7)$$

where $g_1 = -1/\log\{1 - \exp(-1/z_1)\}$, $g_2 = -1/\log\{1 - \exp(-1/z_2)\}$, and the exponent measure V (Padoan et al., 2010) is defined as:

$$V\{g_1, g_2\} = -\frac{1}{g_1}\Phi\left\{\frac{a}{2} + \frac{1}{a}log\frac{g_2}{g_1}\right\} - \frac{1}{g_2}\Phi\left\{\frac{a}{2} + \frac{1}{a}log\frac{g_1}{g_2}\right\}. \qquad (8)$$

In Eq. (8), Φ is the standard normal cumulative distribution function, $a = \sqrt{2\gamma_{ad.}(h)}$ with $\gamma_{ad.}(h)$ is the variograms that was mentioned in the explanation of Eq. (6).

In unit Fréchet margins, the relationship between the return level z and the return period T is given as $z = -1/log(1 - 1/T)$, and the conditional probability for the max-stable process can then be estimated using:

$$P\{Z_2 > z_2 | Z_1 > z_1\} = T_1\left[\frac{1}{T_1} - \exp\left(-\frac{1}{z_2}\right) + P\{Z_1 \le z_1, Z_2 \le z_2\}\right], \qquad (9)$$

where T_1 is the return period corresponding to the return level z_1.

~~This section introduces general concepts for evaluating a conditional probability and a joint probability for a bivariate case. A detailed method is then presented for estimating the conditional probability and the joint probability for the realistic case of rainfall extremes.~~

~~Figure 5 illustrates a bivariate case for two locations~~ $\cancel{x_1}$ ~~and~~ $\cancel{x_2}$ ~~as a scatterplot of events at two locations. The extremes are delineated for each location according to a specified threshold (e.g.~~ $\cancel{u = 0.98}$ ~~percentile) and to distinguish them, colour coding and different symbols have been used. The four regions have been labelled for ease of reference: (A) only~~ $\cancel{Z_2}$ ~~extreme events but not~~ $\cancel{Z_1}$~~, (B) both~~ $\cancel{Z_1}$ ~~and~~ $\cancel{Z_2}$ ~~extreme, (C) only~~ $\cancel{Z_1}$ ~~extreme events but not~~ $\cancel{Z_2}$~~, and (D) non-extreme events.~~

Formatted: Space After: 0 pt, Line spacing: Double

Formatted: Space After: 0 pt, Line spacing: Double

Formatted: Space After: 0 pt, Line spacing: Double

Formatted: Space After: 0 pt, Line spacing: Double

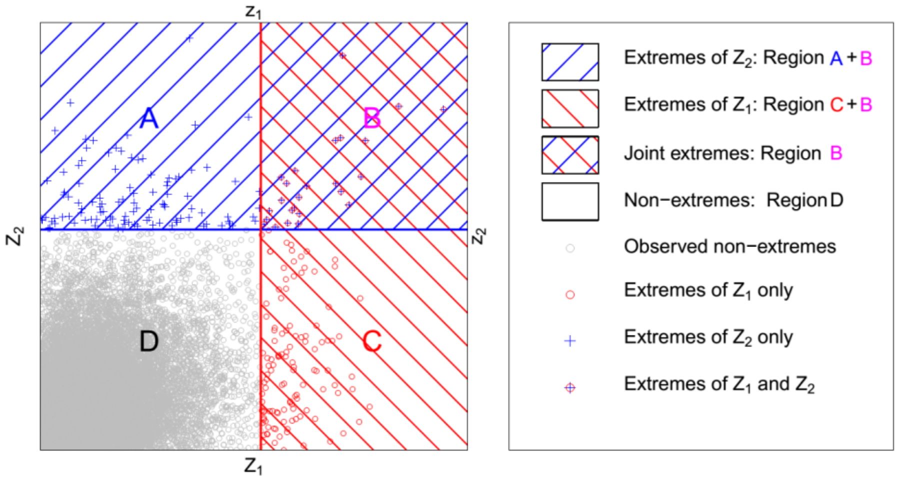

Figure 5. Illustration of general concept of probabilities for a bivariate case. Z_1 and z_1 indicate stochastic process Z and a threshold at location x_1; Z_2 and z_2 indicate stochastic process Z and a threshold at location x_2.

To explain how the joint and conditional probabilities are calculated, their definitions are provided in Table 2 with reference to the regions of Fig. 5. Rather than consider the specific case of a theoretical model of extremal rain (e.g. inverted max stable), Table 2 presents these concepts more simply using only two variables and with generic probability estimates. Equations for both dependence and independence are provided in Table 2.

Table 2. Definition of joint and conditional probabilities and how to calculate them for the case of bivariate independent and dependent variables.

Case	Definition	Calculation
1. Conditional prob. dependent	$P\{Z_2 > z_2 \| Z_1 > z_1\}$	$= P(B)/\{P(B) + P(C)\}$
2. Conditional prob. independent	$P\{Z_2 > z_2 \| Z_1 > z_1\} = P\{Z_2 > z_2\}$	$= P(A) + P(B)$
3. Joint prob. dependent	$P\{Z_1 > z_1, Z_2 > z_2\}$	$= P(B)$
4. Joint prob. independent	$P\{Z_1 > z_1, Z_2 > z_2\} = P\{Z_1 > z_1\} \times P\{Z_2 > z_2\}$	$= \{P(B) + P(C)\}\{P(A) + P(B)\}$

Case 1: Conditional probability can be defined as the joint probability divided by the marginal probability $P\{Z_2 > z_2 | Z_1 > z_1\} = P\{Z_1 > z_1, Z_2 > z_2\}/P\{Z_1 > z_1\}$. For the dependent case, the relationship is $P(B)/\{P(B) + P(C)\}$. Using these concepts, equations for the conditional probability of the inverted max-stable process have been derived in literature and are summarised in Appendix B.

~~The detailed formulae are of the same nature as those in Table 2, and are used in this study to estimate conditional maps for return periods once the model has been fitted to all durations.~~

~~**Case 2:** Using the definition of $P\{Z_2 > z_2 | Z_1 > z_1\} = P\{Z_1 > z_1, Z_2 > z_2\}/P\{Z_1 > z_1\}$ for the independent case results in the exceedance probability for Z_2, which is $P(A) + P(B)$ (since intuitively Z_1 has no effect on exceedances of Z_2).~~

~~**Case 3:** For the case of dependent variables the joint exceedance is defined by $P(B)$. For the case of only two locations, the probability that there is at least one location that has an extreme event exceeding a given threshold is calculated as $P\{Z_1 > z_1 \text{ or } Z_2 > z_2\} = P\{Z_1 > z_1\} + P\{Z_2 > z_2\} - P\{Z_1 > z_1, Z_2 > z_2\}$. Here, $P\{Z_1 > z_1, Z_2 > z_2\}$ can be easily obtained from the bivariate CDF for inverted max-stable process in Eq. (B.1). However, for the case of multiple locations (five different locations for this paper), it is difficult to derive the formula for this probability because there are dependences between extreme events at all locations. So this probability is empirically calculated from a large number of simulations of the dependent model (see the description of the simulation procedure for an inverted max-stable process in Section 4.5). It is also noted that the case study contains five catchments, which have approximate times of concentration of either 36 hr or 9 hrs.~~

~~**Case 4:** Joint probability for~~ The joint probability for independent variables is broken down as the product of the marginals. ~~The exceedance probability for Z_1 is $P(B) + P(C)$ and the exceedance probability for Z_2 is $P(A) + P(B)$, and by definition their independent product will result in the joint probability. In order to compare with a situation of no spatial dependence of rainfall extremes, the~~The probability that there is at least one location that has an extreme event exceeding a given threshold for the case that all of events are independent can be calculated based on the addition rule for the union of probabilities, as:

$$P(Z_1 > z_1 \text{ or} \dots \text{or } Z_N > z_N) = \sum_{i=1}^{N} P(Z_i > z_i) - \sum_{i<j} P\left(Z_i > z_i, Z_j > z_j\right) + \cdots$$

$$+(-1)^{N-1} P(Z_1 > z_1, \dots, Z_N > z_N), \qquad (\cancel{5}10)$$

Formatted: Space After: 10 pt

where $\cancel{N}$$N$ is the number of locations, and $\cancel{P(Z_1 > z_1, \ldots, Z_N > z_N) = P(Z_1 > z_1) \ldots P(Z_N > z_N)}$$P(Z_1 > z_1, \ldots, Z_N > z_N) = P(Z_1 > z_1) \ldots P(Z_N > z_N)$, because all of the events are independent.

4.5. Areal reduction factor estimation and simulation procedure for spatial rainfall

Before ~~being transformed to flood flow through an event-based model, the rainfall extremal estimates need to be converted to the average spatial rainfall using an areal reduction factor (ARF) (Ball et al., 2016).~~transforming extreme rainfall to flood flow through an event-based model, areal reduction factors (ARFs) were employed to make the adjustment of rainfall depth at a point (i.e. the centroid of a catchment) for a given return level estimate, to an effective (mean) depth over a catchment with the same probability of exceedance as the single point (Ball et al., 2016; Le et al., 2018a). ARFs can be estimated from observed rainfall data, but it is difficult to extrapolate ARFs for long return periods from observations with just 35 years of record for this study. To deal with this difficulty and to analyse the asymptotic behaviour of ARFs, ~~Le et al. (2018a)~~Le et al. (2018a) proposed a framework to simulate ARFs for long return periods by using an inverted max-stable process, which is applied here for durations of 36 and 9 hrs.

The simulation procedure for spatial rainfall for a given duration is implemented in two steps. In the first step, the ~~Brown-Resnick process with unit Fréchet margins~~ theoretical residual tail dependence coefficient function in Eq. (5) is fitted to observed rainfall for the duration of interest to obtain the variogram parameters $q > 0$ and $\beta \in (0,2)$. The Brown-Resnick process with unit Fréchet margins is then simulated using the algorithm of ~~Dombry et al. (2016)~~Dombry et al. (2016) over a spatial domain ~~(whether specific locations of interest or grid points), and then~~and the inverted Brown-Resnick process with unit Fréchet margins is obtained through Eq. ~~(4) and Eq. (5) in Le et al. (2018a).~~(2) and Eq. (3). In the second step, the ~~spatial rainfall processes are obtained by transforming the~~ simulation ~~of the inverted Brown-Resnick process~~ in step 1 is transformed from unit Fréchet margins to the rainfall scaled margins~~ using the GP~~. For rainfall magnitudes above the threshold the generalised Pareto distribution in Eq. ~~(1) for rainfall magnitude above the threshold~~(1) is used, and below the threshold the empirical distribution ~~for rainfall magnitude below the threshold.~~ is used. The empirical

Formatted: Font: Not Bold, Not Italic

Formatted: Heading 2, Left, Space Before: 0 pt, Line spacing: single distributions at ungauged sites are derived from the nearest gauged sites using a response surface (latitude and longitude covariates) to spatially interpolate the threshold.

An advantage of this approach is that it can reflect the proportion of dry days in the empirical distribution by making the simulated rainfall contain zero values ~~(Thibaud et al., 2013)~~(Thibaud et al., 2013). Another advantage is that this approach guarantees that the marginal distributions of simulated rainfall below the threshold matches the observed marginal distributions. There may be a drawback of this approach by forcing the simulated rainfall to have the same extremal dependence structure for both parts below and above the threshold, which may not be true for non-extreme rainfall. However, the dependence structure of non-extreme rainfall contributes insignificantly to extreme events ~~(Thibaud et al., 2013)~~(Thibaud et al., 2013) and is unlikely to affect the results.

For calculating ARFs, the simulation is implemented separately for spatial rainfall of 36 and 9 hrs duration. After the simulated spatial rainfall for 36 and 9 hrs are respectively obtained, ARFs are calculated for each duration and different return periods, which can be found in the supplementary material (Fig. S1 and S2). ~~When the interest is in the joint probability of rainfall extremes of different durations (see Case 3 in Section 4.4), the simulation of spatial rainfall should be implemented across multiple durations. In this case, each term of the covariance matrix is calculated from the dependence structure of the corresponding pair of locations.~~ Figure S1 and S2 provide relationships between ARFs and area (in km^2) for different return periods for the case study catchments. These relationships are calculated through the simulation of inverted Brown-Resnick process over equally sized grid points. The relationships are interpolated to obtain the ARFs for each of subcatchments (corresponding to respective areas 91 km^2, 294 km^2, 341 km^2, 771 km^2, 1020 km^2). When the interest is in the joint probability of rainfall extremes of different durations, the simulation of spatial rainfall should be implemented across multiple durations. In this case, each term of the covariance matrix is calculated from the dependence structure of the corresponding pair of locations. In detail, the covariance matrix of the simulation procedure provided by Dombry et al. (2016) is calculated from the variogram in Eq. (6). The covariance element for a pair of locations with the same duration (e.g. 36 and 36 hr) is calculated from the variogram of identical durations for 36 and 36 hr. The covariance element for a pair of locations with different durations (e.g. 36 and 9 hr) is calculated from the variogram across durations for 36 and 9 hr.

4.6. Transforming rainfall extremes to flood flow

To estimate flood flow from rainfall extremes, the Watershed Bounded Network Model (WBNM) ~~(Boyd et al., 1996)~~(Boyd et al., 1996), is employed in this study. WBNM calculates flood runoff from rainfall hyetographs~~.~~ that represent the relationship between the rainfall intensity and time (Chow et al., 1988). It divides the catchment into subcatchments, allowing hydrographs to be calculated at various points within the catchment, and allowing the spatial variability of rainfall and rainfall losses to be modelled. It separates overland flow routing from channel routing, allowing changes to either or both of these processes, for example in urbanised catchments. The rainfall extremes are estimated at the centroid of the catchment, and are converted to average spatial rainfall using the simulated ARFs described in Section 4.5 before estimation of the rainfall hyetographs.

Hydrological models (WBNM) for the case study area were developed and calibrated ~~by engineering consultants (WMAWater, 2011)~~(WMAWater, 2011). ~~As an example, Fig. 6 provides details of the hydrological models~~Hydrological model layouts for the Bellinger ~~catchment and~~ , Kalang River ~~catchment in the North. The plots for details of the hydrological models for the~~, Nambucca ~~basin in the South~~, Warrell and ~~the~~ Deep Creek ~~catchment in the East~~catchments can be found in the supplementary material (Fig. S3 ~~and S4~~to S5).

Formatted: Font: 9 pt

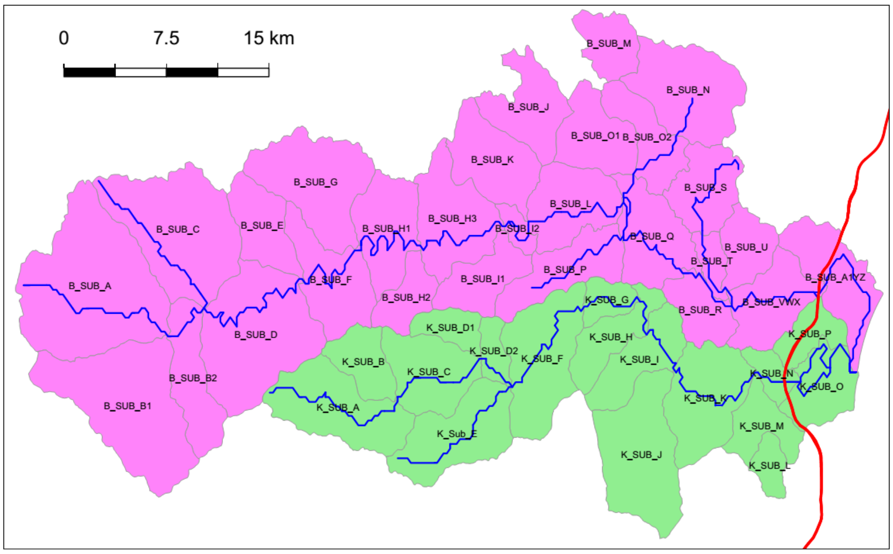

~~**Figure 6.** Hydrological model layout for Bellinger catchment and Kalang River catchment. The blue lines are the river network, and the red line is the Pacific Highway upgrade project.~~

5. Results and discussion

5.1. Evaluation of model for space-duration rainfall process

A GPD with an appropriate threshold was fitted to the observed rainfall data for 36 hr and 9 hr durations, and the Brown-Resnick inverted max-stable process model was calibrated to determine the spatial dependence.

Analysis of the rainfall records led to the selection of a threshold of 0.98 for all records as reasonable across the spatial domain and the GPD was fitted to data above the selected threshold. Figure ~~7~~5 shows QQ plots of the marginal estimates for a representative station for two durations 36 and 9 hr. Overall the quality of fitted distributions is good and plots for all other stations can be found in the supplementary material (Fig. ~~S5~~S6 and S7).

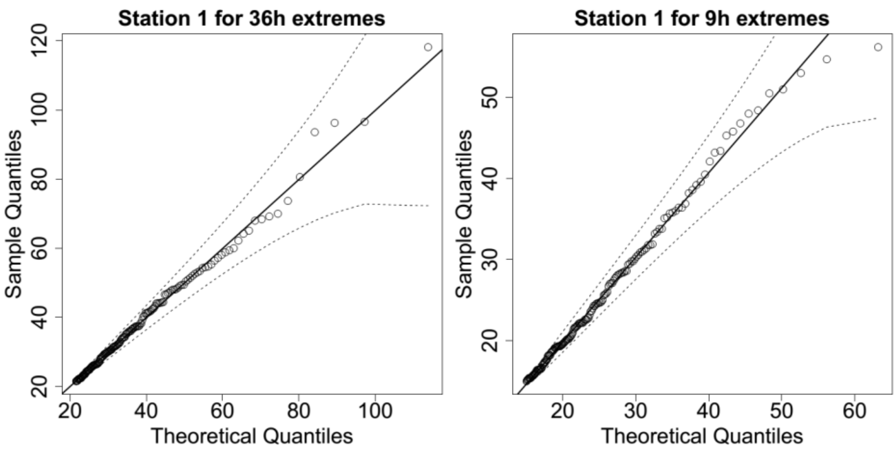

Figure ~~7~~5. QQ plots for the fitted GPD at one representative station, dotted lines are the 95% confidence bounds, and the solid diagonal line indicates a perfect fit.

The inverted max-stable process across different durations was calibrated to determine dependence parameters. The theoretical pairwise residual tail dependence coefficient function between two locations (x_1 and x_2) was calculated based on Eq. (~~3~~5) and Eq. (~~4~~6), and the observed pairwise residual tail dependence coefficient η was calculated using Eq. ~~(2). The model has a reasonable fit to the observed data given the small number of dependence parameters.~~(4). Figure ~~8~~6 shows the pairwise residual tail dependence coefficients for the Brown-Resnick inverted max-stable process versus distance. The black points are the observed pairwise residual tail dependence coefficients, while the red lines are the fitted pairwise residual tail dependence coefficient functions. A coefficient equal to 1 indicates complete spatial dependence, and a value of 0.5 indicates complete spatial independence. The top-left panel shows the dependence between 36 hr extremes across space, with the distance $h = 0$ corresponding to "complete dependence". It also shows the dependence decreasing with increasing distance. Figure 6 indicates that the model has a reasonable fit to the observed data given the small number of dependence parameters. Although the theoretical coefficient (red line) does not perfectly at long distances, the main interest is in short distances, especially at $h = 0$ for the case of dependence between two different durations at the same location.

The remaining panels of Fig. ~~8~~6 show the dependence of 36 vs. 9 hr extremes, 36 vs. 6 hr extremes, and 36 vs. 3 hr extremes, with the latter two duration combinations not being used directly in the study but nonetheless showing the model performance across several durations. As expected, the dependence levels are weaker compared with 36 vs. 36 hr extremes at the same distance, especially at ~~the~~zero distance~~ of 0~~. This is expected, as the dependence at the same site between ~~annual maxima~~exceedances at different durations will be lower than between ~~annual maxima~~exceedances at the same duration. This is because ~~the annual maxima~~exceedances of different durations may arise from different storm events (Zheng et al., 2015).

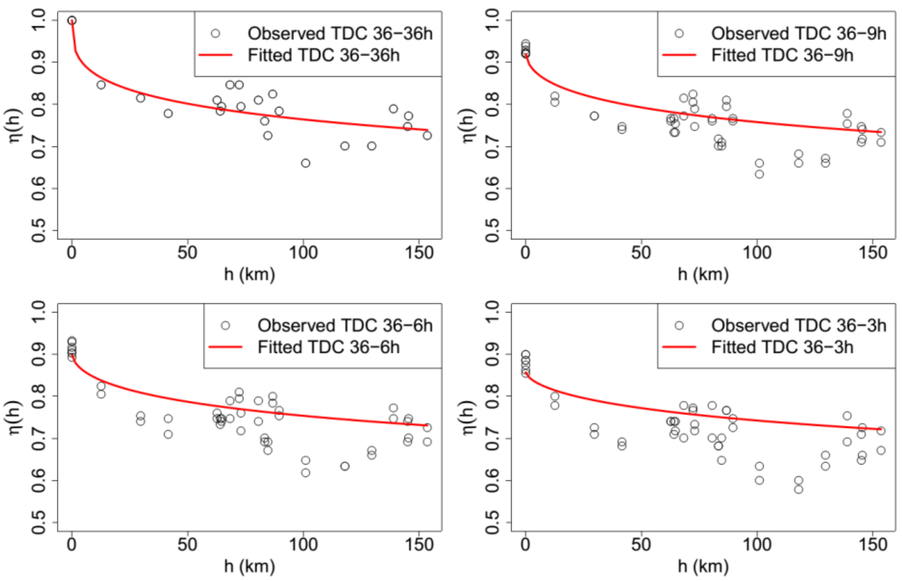

Figure ~~8~~6. Plots of pairwise residual tail dependence coefficient (TDC) against distance for 36 hr extremes and 36 hr extremes (top left), ~~and~~for 36 hr extremes and 9 hr extremes (top right), for 36 hr extremes and ~~9~~6 hr extremes (bottom left), and for 36 hr extremes and 3 hr extremes (bottom right). The black points are estimated residual tail dependence coefficients ~~(TDC)~~ for pairs of sub-daily stations, and the red lines are theoretical residual tail dependence coefficient ~~(TDC)~~ function.

5.2. Estimating conditional rainfall extremes and corresponding conditional flows for evacuation route design

Field Code Changed

Formatted: Underline, Font color: Hyperlink

Formatted: Underline, Font color: Hyperlink

The recommended approach for estimating conditional rainfall extremes is demonstrated by considering a hypothetical evacuation route across location x_2, given a flood occurs at location x_1, evaluated using Eq. (~~B.3~~9). This approach is applied to a case study of the Pacific Highway upgrade project that contains five main river crossings (from Fig. 3). For evacuation purposes, we need to know "what is the probability that a bridge fails only once on average every M times (e.g., $M = 10$ for ~~a 10-year~~an one in 10 chance conditional event) that its neighbouring bridge is flooded?" This section provides the conditional estimates for two pairs of neighbouring bridges in the case study that have the shortest Euclidean distances, i.e. pairs (x_1, x_2) and (x_2, x_3). The comparisons of unconditional and conditional maps are given in Fig. ~~9~~7 and Fig. ~~10~~8, and the corresponding unconditional and conditional flows are given in Fig. ~~11.~~9. In order to obtain the maps in Fig. 7 and Fig. 8, a thin plate spline regression against longitude and latitude was employed to build the response surface for the marginal distribution parameters of rainfall at every pixel.

The left panel of Fig. ~~9~~7 provides the pointwise 10-year unconditional return level map over the case study area for 36 hr rainfall extremes. The value at the location of interest—the blue star (the centroid of Bellinger catchment)—is around 260 mm. The right panel of Fig. ~~9~~7 indicates that when accounting for the effect of a 20-year event for 36 hr rainfall extremes happening at the location of the red star (the centroid of Kalang River catchment), the pointwise one in 10~~-year~~ chance conditional return level at the blue star rises to around 453 mm (i.e., 1.74 times the unconditional value).

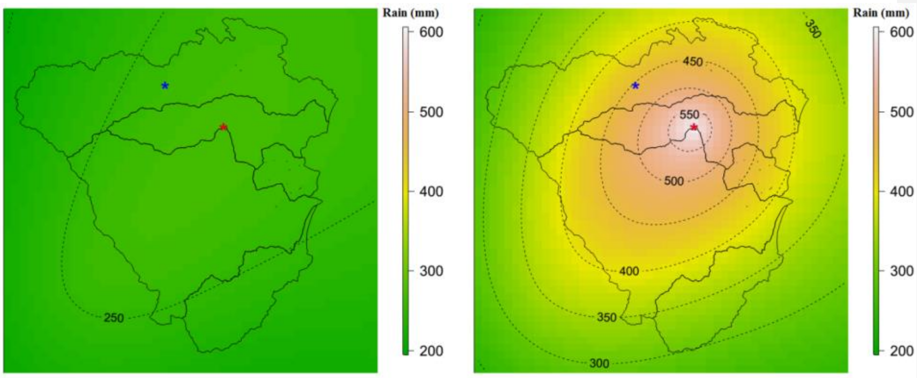

Figure ~~9~~7. Pointwise 10-year unconditional return level map (mm) for 36 hr extremes (left), and pointwise one in 10~~-year~~ chance conditional return level map (mm) for 36 hr extremes given a 20-year event for 36 hr extremes happen at location of the red star for the centroid of Kalang River catchment (right). The colour scales are the same for comparison.

Figure ~~10~~8 provides similar plots to Fig. ~~9~~7 for another pair of locations having different durations of rainfall extremes due to different times of concentration in each catchment. Here, the location of interest is the centroid of the Deep Creek catchment (the blue star in Fig. ~~10~~8) and the conditional point is the centroid of the Kalang River catchment (the red star in Fig. ~~10~~8). The pointwise 10-year unconditional and one in 10 chance conditional return levels at the location of the blue star are 134 mm and 194 mm, respectively. The relative difference between the conditional and unconditional return levels is only 1.45 times, compared with 1.74 times for the case in Fig. ~~9~~7. This is because the pair of locations in Fig. ~~10~~8 has a longer distance than those in Fig. ~~9~~7, so that the dependence level is weaker. Moreover, the location pair in Fig. ~~10~~8 was analysed for different durations (between 36 and 9 hr extremes), which has weaker dependence than the case of the equivalent durations in Fig. ~~9~~7 (between 36 and 36 hr), based on Fig. ~~8~~6.

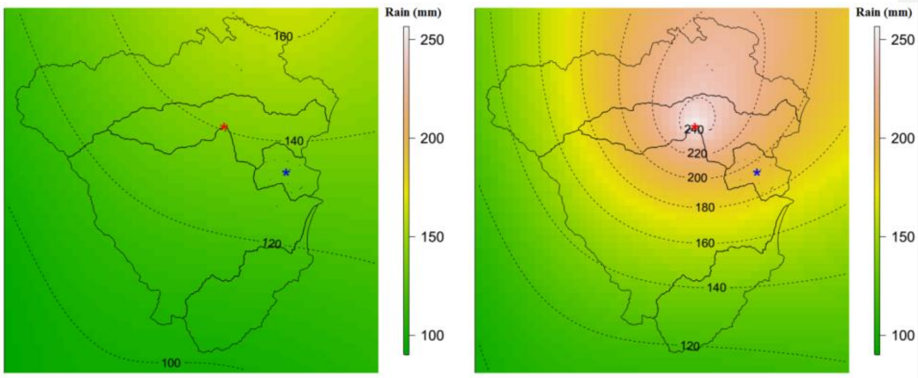

Figure ~~10~~8. Pointwise 10-year unconditional return level map (mm) for 9 hr extremes (left), and pointwise one in 10~~-year~~ chance conditional return level map (mm) for 9 hr extremes, given a 20-year event for 36 hr extremes happens at location of the red star for the centroid of the Kalang River catchment (right). The colour scales are the same for comparison.

The unconditional and conditional return levels are transformed to flood flows via the hydrological model WBNM previously calibrated to each catchment ~~(WMAWater, 2011)~~(WMAWater, 2011). The unconditional and conditional return levels were extracted at the centroid of each main catchment, which were then converted to the average spatial rainfall using an areal reduction factor (ARF). The corresponding unconditional and conditional flood flows at the river crossing in the Bellinger catchment (corresponding to the unconditional and conditional rainfall extremes in Fig. ~~9~~7) are given in Fig. ~~11~~9 (left panel). Similar plots for the river crossing in the Deep Creek catchment (corresponding to the unconditional and conditional rainfall extremes in Fig. ~~10~~8) are given in Fig. ~~11~~9 (right panel).

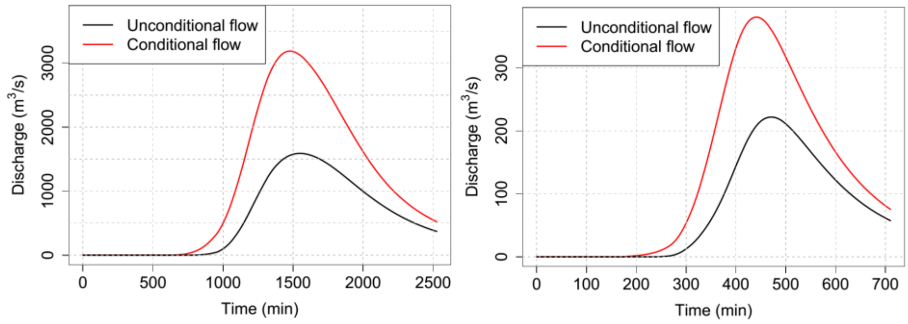

Figure ~~11~~9. Comparison between conditional flows (red line) and unconditional flows (black line). (left) At the river crossing in the Bellinger catchment~~:~~ (number 1 in Figure 3): conditional flow caused by ~~a~~an one in 10 ~~year~~chance conditional event for 36 hr rainfall in considering the effect of a 20~~-~~-year event for 36 hr rainfall occurring at the river crossing in the Kalang River catchment, and unconditional flow caused by a 10-year unconditional event for 36 hr. (right) At the river crossing in the Deep Creek catchment (number 3 in Figure 3): conditional flow caused by an one in 10 chance conditional event for 9 hr rainfall in considering the effect of a 20-year event for 36 hr rainfall occurring at the river crossing in the Kalang River catchment, and unconditional flow caused by a 10~~-year unconditional event for 36 hr. (right) At the river crossing in the Deep Creek catchment: conditional flow caused by a 10 year conditional event for 9 hr rainfall in considering the effect of a 20 year event for 36 hr rainfall occurring at the river crossing in the Kalang River catchment, and unconditional flow caused by a 10~~ -year unconditional event for 9 hr rainfall.

The left panel of Fig. ~~11~~9 indicates that the peak conditional flow at the river crossing in the Bellinger catchment is almost 2.0 times higher than that for unconditional flow. The time taken to reach to the peaks is the same for both cases. This is because this river crossing is affected by a large region with a long time of concentration (36 hr); the impact of rainfall losses on the hydrograph is insignificant. This difference is a direct result of the conditional relationship being more stringent than the unconditional relationship. Given that there is an existing extreme event nearby, it is more likely for an extreme event to occur at another location of interest in the region. If a bridge design were to take into account this extra criterion for the purposes of evacuation planning it would require the design to be at a higher level.

Shown in the right panel in Fig. ~~11~~9, the peak of the conditional flow at the river crossing in the Deep Creek catchment occurred earlier, and is around 1.7 times higher than that for the unconditional flow. This is due to the fact that the river crossing in Deep Creek covers a small region with a short time of concentration (9 hr) and the impact of rainfall losses on the hydrograph is significant.

Although Fig. ~~11~~9 shows a difference in terms of the time taken to reach the peak flows, the two design hydrographs are separate and this is not a physical timing difference. ~~The relevant feature of the conditional design hydrograph is the peak, and timing information is not a part of the method.~~

Formatted: Font: 9 pt

~~The difference between the maximum discharge of conditional and unconditional flows at the river crossing in the Bellinger catchment is shown in Fig. 12 for the case of a 20-year event occurring in the Kalang River catchment nearby. The relationship with AEP indicates that the difference between the maximum discharge of conditional and unconditional flows decreases when AEP increases, and that the difference approaches zero when the AEP increases to above 50% (i.e. a 2-year return period).~~

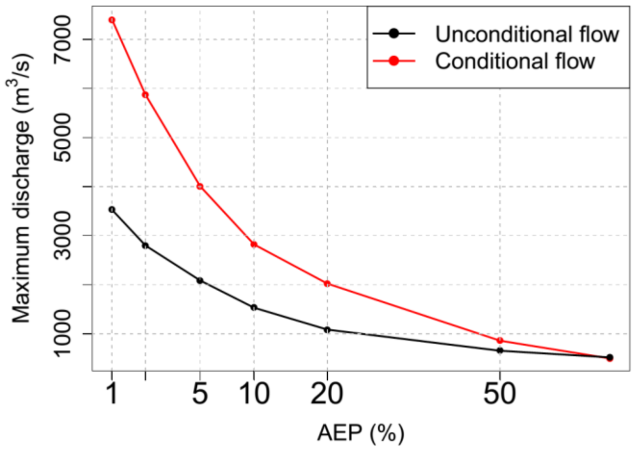

~~**Figure 12.** Plot for peak of conditional flow (red points) caused by conditional flood-producing rainfall and peak of unconditional flow (black points) for different annual exceedance probabilities (AEP) at the river crossing in the Bellinger catchment. This plot considers the effect of a 20-year event occurring at the river crossing in the Kalang River catchment.~~

5.3. Estimating the failure probability of the highway section based on the joint probability of rainfall extremes

The recommended approach for estimating the overall failure probability of a system is demonstrated by considering a hypothetical traffic system with multiple river crossings at locations $x_1, \ldots, x_N$. If there is a one-to-one correspondence between extreme rainfall intensity over a catchment and flood magnitude, the overall failure probability will be approximately equal to the probability that there is at least one river crossing whose contributing catchment has rainfall extremes exceeding the design level, which can be estimated using a large number of simulations from the spatial rainfall model. This approach is applied to the Pacific Highway upgrade project containing five river crossings. A set of 10,000 year simulated rainfall (Section 4.5) is generated from the fitted model (Section 5.1) to calculate the overall failure probability of the highway section. This process is repeated 100 times to estimate the average failure probability, under the assumption that all river crossings are designed to the same individual failure probability.

Figure ~~13~~10 is a plot of the overall failure probability of the highway ~~and~~as a function of the failure probability of each individual river crossing (black). Similar relationships for the cases of complete dependence (blue) and complete independence (red) are also provided for comparison. For the case of complete dependence, when the whole region is extreme at the same time, the overall failure probability of the highway is equal to the individual river crossing failure probability and it represents the best case~~.~~ (the lowest overall failure probability). The worst case is complete independence where extremes do not happen together unless by random chance; this means the failure probability of the highway is much higher than that for individual river crossings. Taking into account the real dependence, there are some extremes that align and it seems from the Fig. ~~13~~10 that this is a relatively weak effect. As an example from Fig. ~~13~~10, to design the highway with a failure probability of 1%

~~annual exceedance probability (~~AEP~~)~~, we would have to design each individual river crossing to a much rarer AEP of 0.25% (see green lines in Fig. ~~13~~10).

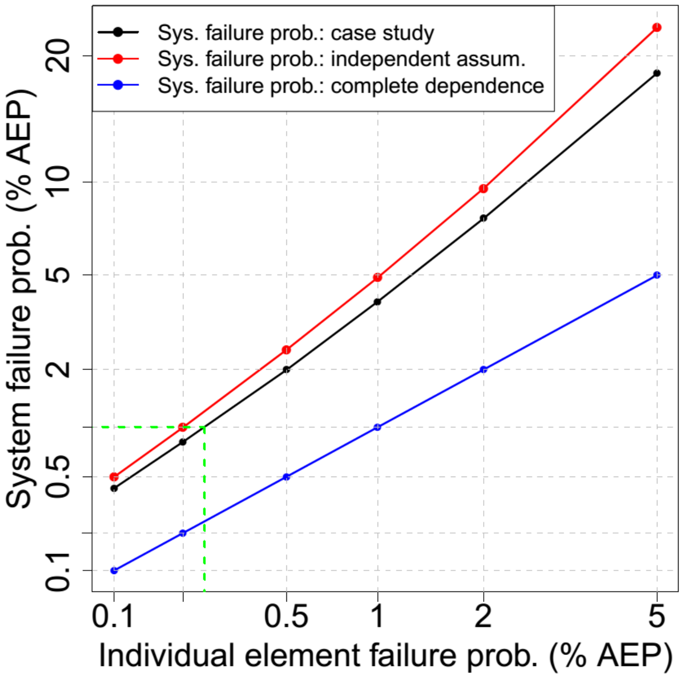

Figure ~~13~~10. Relationship between system failure probability and individual element failure probability in % annual exceedance probability (% AEP). The black colour is for the case study, the red colour is for the case of complete independence, and the blue is for the case of complete dependence. The green lines help to interpolate the individual element failure probability from a given system failure probability of 1%. Both horizontal axis and vertical axis are constructed at a double log scale for viewing purposes.

6. Discussion and Conclusions

Hydrological design, that is based on IDF curves, has conventionally focussed on individual catchments and individual extremes. Such an approach can lead to an underestimation of wider system risk of flooding since weather systems exhibit dependence in space and time, which can lead to the coincidence of extremes. A number of methods have been developed to address the problem of antecedent moisture within a single catchment, by accounting for the temporal dependence of rainfall at locations of interest through loss parameters or sampling rainfall patterns ~~(Rahman et al., 2002)~~(Rahman et al., 2002). However, there have been fewer methods that account for the spatial dependence of rainfall across multiple catchments, due in part to the complexity of representing the effects of spatial dependence in risk calculations. Different catchments can have different times of concentration, so spatial dependence may also imply the need to consider dependence across different durations of extreme rainfall bursts.

Recent and ongoing advances in modelling spatial rainfall extremes provide an opportunity to revisit the scope of hydrological design. Such models include a max-stable model fitted using a Bayesian hierarchical approach ~~(Stephenson et al., 2016)~~(Stephenson et al., 2016), max-stable and inverted max-stable models ~~(Nicolet et al., 2017; Padoan et al., 2010; Russell et al., 2016; Thibaud et al., 2013; Westra and Sisson, 2011)~~(Nicolet et al., 2017; Padoan et al., 2010; Russell et al., 2016; Thibaud et al., 2013; Westra and Sisson, 2011) and latent-variable Gaussian models ~~(Bennett et al., 2016b)~~(Bennett et al., 2016b). The ability to simulate rainfall over a region means that hydrological problems need not be confined to individual catchments, but may cover multiple catchments. Civil infrastructure systems such as highways, railways or levees are such examples, since the failure of any one element may lead to overall failure of the system. Alternatively, where there is a network, the failure of one element may have implications for the overall system to accommodate the loss, by considering alternative routes. With models of spatial dependence and duration dependence of extremes there is a new and improved ability to address these problems explicitly as part of the design methodology.

This paper demonstrated an application for evaluating conditional and joint probabilities of flood at different locations. This was achieved with two examples: (i) the design of a river crossing that will fail once on average every M times given that its neighbouring river crossing is flooded; and (ii) estimating the probability that a highway section, which contains multiple river crossings, will fail based on the failure probability of each individual river crossing. Due to the lack of continuous streamflow data and subdaily limitations of rain-based continuous simulation, this study used an event-based method of conditional and joint rainfall extremes to estimate the corresponding conditional and joint flood flows. The spatial rainfall was simulated using an asymptotically independent model, which was then used to estimate conditional and joint rainfall extremes. ~~An empirical method was obtained from the framework of Le et al. (2018b)~~An empirical method was obtained from the framework of Le et al. (2018b) to make an asymptotically independent model—the inverted max-stable process—able to capture the spatial dependence of rainfall extremes across different durations. The fitted residual tail dependence coefficient function showed that the model can capture the dependence for different pairs of durations. For our example, the highest ratio of the one in 10 chance conditional event (in considering the effect of a 20-year event rainfall occurring at the conditional location) to the 10-year unconditional ~~extremes~~event was 1.74, for the two catchments having the strongest dependence (Fig. ~~9~~7). The corresponding conditional flows were then estimated using a hydrological model WBNM and shown to be strongly related to the ratio of conditional and unconditional rainfall extremes (Fig. ~~11~~9).

The joint probability of rainfall extremes for all catchments and for all possible pairs of catchments in the case study area was estimated empirically from a set of 10,000 years of simulated rainfall extremes, repeated 100 times to estimate the average value. The results showed that there were differences in the failure probability of the highway after taking into account the rainfall dependence, but the effect was not as emphatic as with the case of conditional probabilities. The difference in the failure probability became weaker as the return period increased, which is consistent with the characteristic of asymptotically independent data ~~(Ledford and Tawn, 1996; Wadsworth and Tawn, 2012)~~(Ledford and Tawn, 1996; Wadsworth and Tawn, 2012). A relationship was demonstrated (Fig. ~~13~~10) to show how the design of the overall system to a given failure probability requires the design of each individual river crossing to a rarer extremal level than when each crossing is considered in isolation. For the case study example, it would be necessary to design each bridge to a 0.25% AEP event in order to obtain a system failure probability of 1%.

There is a need to reimagine the role of intensity-duration-frequency curves. Conventionally they have been developed as maps of the marginal rainfall in a point-wise manner for all locations and for a range of frequencies and durations. The increasing sophistication of mathematical models for extremes, computational power and interactive graphics abilities of online mapping platforms means that analysis of hydrological extremes could significantly expand in scope. With an underlying model of spatial and duration dependence between the extremes, it is not difficult to conceive of digital maps that dynamically transform from the marginal representation of extremes to the corresponding representation conditional extremes after any number of conditions are applied. This transformation is exemplified by the differences between left and right panels in Fig. ~~9~~7 and Fig. ~~10~~8. Enhanced IDF maps would enable a very different paradigm of design flood risk estimation, breaking away from analysing individual system elements in isolation to emphasize the behaviour of entire system.

Appendix A. Calculation of empirical tail dependence coefficient

To illustrate how Eq. (~~2~~4) in the manuscript is calculated, consider a set of $n = 10$ observed values at the two locations:~~$Z_1 = c(5,9,1,2,10,3,8,6,4,7)$;~~ Z_1 and Z_2 ~~$= c(10,1,7,6,4,3,9,2,8,5)$.~~ (see Table A1). First, Z_1 and Z_2 are converted to empirical cumulative probability estimates via the Weibull plotting position formula $P = j/(n+1)$ where j is ranked index of a data point giving P_1 ~~$= c(0.455, 0.818, 0.091, 0.182, 0.909, 0.273, 0.727, 0.545, 0.364, 0.636)$ and $P_2 = c(0.909, 0.091, 0.636, 0.545, 0.364, 0.273, 0.818, 0.182, 0.727, 0.455)$.~~ and P_2 (see Table A1).

Table A1. Observed data Z_1 and Z_2 and corresponding empirical cumulative probabilities P_1 and P_2.

Z_1	Z_2	P_1	P_2
5	10	0.455	0.909
9	1	0.818	0.091
1	7	0.091	0.636
2	6	0.182	0.545
10	4	0.909	0.364
3	3	0.273	0.273
8	9	0.727	0.818
6	2	0.545	0.182
4	8	0.364	0.727
7	5	0.636	0.455

Assume that interest is in values above a threshold $u = 0.5$, in other words, $P\{Z_2 > z\} = P\{P_2 > u\} = 0.5$. In this case we have only one pair, at the index of 7, that satisfy both P_1 and P_2 are greater than $u = 0.5$, thus $P\{Z_1 > z, Z_2 > z\} = P\{P_1 > u, P_2 > u\} = 1/10 = 0.1$. The calculation of the empirical tail dependence coefficient is then

$$\eta(x_1, x_2) = \frac{\log P\{Z_2 > z\}}{\log P\{Z_1 > z, Z_2 > z\}} = \frac{\log P\{P_2 > u\}}{\log P\{P_1 > u, P_2 > u\}} = \frac{\log(0.5)}{\log(0.1)} = 0.301. \qquad (A.1)$$

~~**Appendix B. Equations for bivariate conditional and joint probabilities for inverted max-stable**~~

~~In the context of this study, the conditional probability $P\{Z_2 > z_2 | Z_1 > z_1\}$ is obtained from the bivariate inverted max-stable process cumulative distribution function (CDF) in unit Fréchet margins (Thibaud et al., 2013), which is given as:~~

$$P\{Z_1 \leq z_1, Z_2 \leq z_2\} = 1 - \exp\left\{-\frac{1}{g_1}\right\} - \exp\left\{-\frac{1}{g_2}\right\} + \exp[-V\{g_1, g_2\}], \qquad (\cancel{B.1})$$

Formatted: Space Before: 6 pt, After: 0 pt

Formatted: Space After: 0 pt, Line spacing: Double

~~where $g_1 = -1/\log\{1-\exp(-1/z_1)\}$, $g_2 = -1/\log\{1-\exp(-1/z_2)\}$, and the exponent measure V (Padoan et al., 2010) is defined as:~~

$$V\{g_1, g_2\} = -\frac{1}{g_1}\Phi\left\{\frac{a}{2} + \frac{1}{a}log\frac{g_2}{g_1}\right\} - \frac{1}{g_2}\Phi\left\{\frac{a}{2} + \frac{1}{a}log\frac{g_1}{g_2}\right\}. \qquad (\cancel{B.2})$$

~~In Eq. (B.2), Φ is the standard normal cumulative distribution function, $a = \sqrt{2\gamma_{aa}(h)}$ with $\gamma_{aa}(h)$ is the variograms that was mentioned in the explanation of Eq. (4) in the manuscript.~~

Formatted: Space After: 0 pt, Line spacing: Double

~~In unit Fréchet margins, the relationship between the return level z and the return period T is given as $z = -1/log(1-1/T)$, and the conditional probability for the max-stable process can then be estimated using:~~

Formatted: Space After: 0 pt, Line spacing: Double

$$P\{Z_2 > z_2 | Z_1 > z_1\} = T_1\left[\frac{1}{T_1} - \exp\left(-\frac{1}{z_2}\right) + P\{Z_1 \le z_1, Z_2 \le z_2\}\right], \qquad (\cancel{B.3})$$

~~where T_1 is the return period corresponding to the return level z_1.~~

Formatted: Space After: 0 pt, Line spacing: Double

Acknowledgments

The lead author was supported by the Australia Awards Scholarships (AAS) from Australia Government. A/Prof Westra was supported by Australian Research Council Discovery grant DP150100411. We thank Mark Babister and Isabelle Testoni of WMA Water for providing the hydrologic models for the case study; and Leticia Mooney for her editorial help in improving this manuscript. The rainfall data used in this study were provided by the Australian Bureau of Meteorology, and can be obtained from the corresponding author.

References

Asadi, P., Davison, A. C., and Engelke, S.: Extremes on river networks, Ann. Appl. Stat., 9, 2023-2050, 10.1214/15-AOAS863, 2015.

Ball, J., Babister, M., Nathan, R., Weeks, W., Weinmann, E., Retallick, M., and Testoni, I.: Australian Rainfall and Runoff: A Guide to Flood Estimation, © Commonwealth of Australia (Geoscience Australia), 2016.

Bárdossy, A., and Pegram, G. G. S.: Copula based multisite model for daily precipitation simulation, Hydrol. Earth Syst. Sci., 13, 2299-2314, 10.5194/hess-13-2299-2009, 2009.

Baxevani, A~~.~~., and Lennartsson, J.: A spatiotemporal precipitation generator based on a censored latent Gaussian field, Water Resources Research, 51, 4338-4358, doi:10.1002/2014WR016455, 2015.

Bennett, B., Lambert, M., Thyer, M., Bates, B. C., and Leonard, M.: Estimating Extreme Spatial Rainfall Intensities, Journal of Hydrologic Engineering, 21, 04015074, doi:10.1061/(ASCE)HE.1943-5584.0001316, 2016a.

Bennett, B., Thyer, M., Leonard, M., Lambert, M., and Bates, B.: A comprehensive and systematic evaluation framework for a parsimonious daily rainfall field model, Journal of Hydrology, ~~doi:~~ https://doi.org/10.1016/j.jhydrol.2016.12.043, 2016b.~~ 2016b.~~

Bernard, M. M.: Formulas for rainfall intensities of long duration, Transactions of the American Society of Civil Engineers, 96, 592-606, 1932.

Boughton, W~~.~~., and Droop, O.: Continuous simulation for design flood estimation—a review, Environmental Modelling & Software, 18, 309-318, ~~2003.~~https://doi.org/10.1016/S1364-8152(03)00004-5, 2003.

Boyd, M. J., Rigby, E. H., and VanDrie, R.: WBNM — a computer software package for flood hydrograph studies, Environmental Software, 11, 167-172, ~~1996.~~https://doi.org/10.1016/S0266-9838(96)00042-1, 1996.

Brown, B. M~~.~~., and Resnick, S. I.: Extreme Values of Independent Stochastic Processes, Journal of Applied Probability, 14, 732-739, 10.2307/3213346, 1977.

Cameron, D. S., Beven, K. J., Tawn, J., Blazkova, S., and Naden, P.: Flood frequency estimation by continuous simulation for a gauged upland catchment (with uncertainty), Journal of Hydrology, 219, 169-187, ~~1999.~~https://doi.org/10.1016/S0022-1694(99)00057-8, 1999.

Carreau, J., Neppel, L., Arnaud, P., and Cantet, P.: Extreme Rainfall Analysis at Ungaug ed Sites in the South of France : Comparison of Three Approaches, Jour nal de la Société Française de Statistique, 154 No. 2, 119-138, 2013.

Chow, V. T., Maidment, D. R., and Mays, L. W.: Applied Hydrology, McGraw-Hill, c1988, New York, 1988.

Coles, S~~.: An Introduction to Statistical Modeling of Extreme Values, Springer, 2001.~~

~~Coles, S~~., Heffernan, J., and Tawn, J.: Dependence Measures for Extreme Value Analyses, Extremes, 2, 339-365, 10.1023/a:1009963131610, 1999.

Coles, S.: An Introduction to Statistical Modeling of Extreme Values, Springer Series in Statistics, Springer, 2001.

Davison, A. C~~.~~., and Smith, R. L.: Models for exceedances over high thresholds, Journal of the Royal Statistical Society. Series B (Methodological), ~~1990.~~ 393-442, 1990.

de Haan, L.: A Spectral Representation for Max-stable Processes, The Annals of Probability, 12, 1194-1204, 10.2307/2243357, 1984.

Demarta, S., and McNeil, A. J.: The t Copula and Related Copulas, International Statistical Review / Revue Internationale de Statistique, 73, 111-129, 2005.

Dombry, C., Engelke, S., and Oesting, M.: Exact simulation of max-stable processes, Biometrika, 103, 303-317, 2016.

Durocher, M., Chebana, F., and Ouarda, T. B. M. J.: On the prediction of extreme flood quantiles at ungauged locations with spatial copula, Journal of Hydrology, 533, 523-532, https://doi.org/10.1016/j.jhydrol.2015.12.029, 2016.

Favre, A. C., Adlouni, S. E., Perreault, L., Thiémonge, N., and Bobée, B.: Multivariate hydrological frequency analysis using copulas, Water Resources Research, 40, doi:10.1029/2003WR002456, 2004.

Formatted: Underline, Font color: Hyperlink

Formatted: Underline, Font color: Hyperlink

Gupta, A. S., and Tarboton, D. G.: A tool for downscaling weather data from large-grid reanalysis products to finer spatial scales for distributed hydrological applications, Environmental Modelling & Software, 84, 50-69, https://doi.org/10.1016/j.envsoft.2016.06.014, 2016.

He, Y., Bárdossy, A., and Zehe, E.: A review of regionalisation for continuous streamflow simulation, Hydrology and Earth System Sciences, 15, 3539, 2011.

Hegnauer, M., Beersma, J., Van den Boogaard, H., Buishand, T., and Passchier, R.: Generator of Rainfall and Discharge Extremes (GRADE) for the Rhine and Meuse basins; Final report of GRADE 2.0, Document extern project, 2014.

Hosking, J. R. M., and Wallis, J. R.: Regional Frequency Analysis - An Approach Based on L-Moments, Cambridge University Press, Cambridge, UK, 1997.

Huser, R~~.~~., and Davison, A. C.: Composite likelihood estimation for the Brown–Resnick process, Biometrika, 100, 511-518, 10.1093/biomet/ass089, 2013.

Hüsler, J., and Reiss, R.-D.: Maxima of normal random vectors: Between independence and complete dependence, Statistics & Probability Letters, 7, 283-286, https://doi.org/10.1016/0167-7152(89)90106-5, 1989.

Kabluchko, Z., Schlather, M., and de Haan, L.: Stationary Max-Stable Fields Associated to Negative Definite Functions, The Annals of Probability, 37, 2042-2065, 2009.

Kao, S.-C~~.~~., and Govindaraju, R. S.: Trivariate statistical analysis of extreme rainfall events via the Plackett family of copulas, Water Resources Research, 44, doi:10.1029/2007WR006261, 2008.

Kleiber, W., Katz, R. W., and Rajagopalan, B.: Daily spatiotemporal precipitation simulation using latent and transformed Gaussian processes, Water Resources Research, 48, doi:10.1029/2011WR011105, 2012.

Koutsoyiannis, D., Kozonis, D., and Manetas, A.: A mathematical framework for studying rainfall intensity-duration-frequency relationships, Journal of Hydrology, 206, 118-135, ~~1998.~~http://dx.doi.org/10.1016/S0022-1694(98)00097-3, 1998.

Kuichling, E.: The relation between the rainfall and the discharge of sewers in populous districts, Transactions of the American Society of Civil Engineers, 20, 1-56, 1889.

Laurenson, E. M~~.~~., and Mein, R. G.: RORB Version 4 Runoff Routing Program User Manual, Monash University Department of Civil Engineering, 1997.

Le, P. D., Davison, A. C., Engelke, S., Leonard, M., and Westra, S.: Dependence properties of spatial rainfall extremes and areal reduction factors, Journal of Hydrology, ~~Submitted,~~565, 711-719, https://doi.org/10.1016/j.jhydrol.2018.08.061, 2018a.

Le, P. D., Leonard, M., and Westra, S.: Modeling Spatial Dependence of Rainfall Extremes Across Multiple Durations, Water Resources Research, 54, 2233-2248, doi:10.1002/2017WR022231, 2018b.

Ledford, A. W~~.~~., and Tawn, J. A.: Statistics for Near Independence in Multivariate Extreme Values, Biometrika, 83, 169-187, 1996.

Leonard, M., Lambert, M. F., Metcalfe, A. V., and Cowpertwait, P. S. P.: A space-time Neyman–Scott rainfall model with defined storm extent, Water Resources Research, 44, doi:10.1029/2007WR006110, 2008.

Leonard, M., Westra, S., Phatak, A., Lambert, M., Hurk, B. v. d., McInnes, K., Risbey, J., Schuster, S., Jakob, D., and Stafford-Smith, M.: A compound event framework for understanding extreme impacts, Wiley Interdisciplinary Reviews: Climate Change, 5, 113-128, doi:10.1002/wcc.252, 2014.

Mulvaney, T. J.: On the use of self-registering rain and flood gauges in making observation of the relation of rainfall and floods discharges in a given catchment, Proc. Civ. Eng. Ireland, 4, 18–31, 1851.

Nicolet, G., Eckert, N., Morin, S., and Blanchet, J.: A multi-criteria leave-two-out cross-validation procedure for max-stable process selection, Spatial Statistics, 22, 107-128, ~~2017.~~https://doi.org/10.1016/j.spasta.2017.09.004, 2017.

Oesting, M., Schlather, M., and Friederichs, P.: Statistical post-processing of forecasts for extremes using bivariate Brown-Resnick processes with an application to wind gusts, Extremes, 20, 309-332, 10.1007/s10687-016-0277-x, 2017.

Opitz, T.: Extremal t processes: Elliptical domain of attraction and a spectral representation, Journal of Multivariate Analysis, 122, 409-413, https://doi.org/10.1016/j.jmva.2013.08.008, 2013.

Padoan, S. A., Ribatet, M., and Sisson, S. A.: Likelihood-Based Inference for Max-Stable Processes, Journal of the American Statistical Association, 105, 263-277, 10.1198/jasa.2009.tm08577, 2010.

Formatted: Hyperlink

Formatted: EndNote Bibliography, Left

Pathiraja, S., Westra, S., and Sharma, A.: Why continuous simulation? The role of antecedent moisture in design flood estimation, Water Resources Research, 48, doi:10.1029/2011WR010997, 2012.

Pickands, J.: Statistical Inference Using Extreme Order Statistics, The Annals of Statistics, 3, 119-131, 10.2307/2958083, 1975.

Rahman, A., Weinmann, P. E., Hoang, T. M. T., and Laurenson, E. M.: Monte Carlo simulation of flood frequency curves from rainfall, Journal of Hydrology, 256, 196-210, ~~2002.~~https://doi.org/10.1016/S0022-1694(01)00533-9, 2002.

Rasmussen, P. F.: Multisite precipitation generation using a latent autoregressive model, Water Resources Research, 49, 1845-1857, doi:10.1002/wrcr.20164, 2013.

Renard, B., and Lang, M.: Use of a Gaussian copula for multivariate extreme value analysis: Some case studies in hydrology, Advances in Water Resources, 30, 897-912, http://dx.doi.org/10.1016/j.advwatres.2006.08.001, 2007.

Requena, A. I., Chebana, F., and Ouarda, T. B. M. J.: A functional framework for flow-duration-curve and daily streamflow estimation at ungauged sites, Advances in Water Resources, 113, 328-340, https://doi.org/10.1016/j.advwatres.2018.01.019, 2018.

Russell, B. T., Cooley, D. S., Porter, W. C., and Heald, C. L.: Modeling the spatial behavior of the meteorological drivers' effects on extreme ozone, Environmetrics, 27, 334-344, doi:10.1002/env.2406, 2016.

Schlather, M.: Models for Stationary Max-Stable Random Fields, Extremes, 5, 33-44, 10.1023/A:1020977924878, 2002.

Seneviratne, S. I., Nicholls, N., Easterling, D., Goodess, C. M., Kanae, S., Kossin, J., Luo, Y., Marengo, J., McInnes, K., and Rahimi, M.: Managing the Risks of Extreme Events and Disasters to Advance Climate Change Adaptation: Changes in Climate Extremes and their Impacts on the Natural Physical Environment, 2012.

~~SKM~~Nambucca Heads Flood Study: http://www.nambucca.nsw.gov.au/cp_content/resources/16152_2011__Nambucca_Heads_Flood_Study_Final_Draft_Chapter_6a.pdf, 2011.

Stedinger, J., Vogel, R., and Foufoula-Georgiou, E.: Frequency Analysis of Extreme Events~~. In~~, in: Handbook of Hydrology, edited by: Maidment, D. R~~. (Ed.),~~., McGraw-Hill, New York, 18.11-18.66, 1993.

Stephenson, A. G., Lehmann, E. A., and Phatak, A.: A max-stable process model for rainfall extremes at different accumulation durations, Weather and Climate Extremes, 13, 44-53, ~~2016.~~https://doi.org/10.1016/j.wace.2016.07.002, 2016.

Thibaud, E., Mutzner, R., and Davison, A. C.: Threshold modeling of extreme spatial rainfall, Water Resources Research, 49, 4633-4644, 10.1002/wrcr.20329, 2013.

Wadsworth, J. L~~.~~., and Tawn, J. A.: Dependence modelling for spatial extremes, Biometrika, 99, 253-272, 10.1093/biomet/asr080, 2012.

Wang, Q. J.: A Bayesian Joint Probability Approach for flood record augmentation, Water Resources Research, 37, 1707-1712, 10.1029/2000WR900401, 2001.

Wang, Q. J., Robertson, D. E., and Chiew, F. H. S.: A Bayesian joint probability modeling approach for seasonal forecasting of streamflows at multiple sites, Water Resources Research, 45, doi:10.1029/2008WR007355, 2009.

Wang, X., Gebremichael, M., and Yan, J.: Weighted likelihood copula modeling of extreme rainfall events in Connecticut, Journal of Hydrology, 390, 108-115, ~~2010.~~http://dx.doi.org/10.1016/j.jhydrol.2010.06.039, 2010.

Westra, S~~.~~., and Sisson, S. A.: Detection of non-stationarity in precipitation extremes using a max-stable process model, Journal of Hydrology, 406, 119-128, ~~2011.~~http://dx.doi.org/10.1016/j.jhydrol.2011.06.014, 2011.

WMAWater: Review of Bellinger, Kalang and Nambucca River Catchments Hydrology, Bellingen Shire Council, Nambucca Shire Council, New South Wales Government, 2011.

Zhang, L~~.~~., and Singh, V. P.: Gumbel–Hougaard Copula for Trivariate Rainfall Frequency Analysis, Journal of Hydrologic Engineering, 12, 409-419, ~~2007.~~doi:10.1061/(ASCE)1084-0699(2007)12:4(409), 2007.

Formatted: Underline, Font color: Hyperlink

Formatted: Underline, Font color: Hyperlink

Zheng, F., Westra, S., and Leonard, M.: Opposing local precipitation extremes, Nature Clim. Change, 5, 389-390, ~~2015.~~10.1038/nclimate2579

http://www.nature.com/nclimate/journal/v5/n5/abs/nclimate2579.html#supplementary-information, 2015.

Zscheischler, J., Westra, S., van den Hurk, B. J. J. M., Seneviratne, S. I., Ward, P. J., Pitman, A., AghaKouchak, A., Bresch, D. N., Leonard, M., Wahl, T., and Zhang, X.: Future climate risk from compound events, Nature Climate Change, 8, 469-477, 10.1038/s41558-018-0156-3, 2018.

Formatted: Space After: 10 pt